NUTRIENT SENSING MECHANISMS IN THE SMALL INTESTINE:

Localisation of taste molecules in mice and humans with and without diabetes

Kate Sutherland, B.Sc. (Hons)

A thesis submitted in fulfilment of the Degree of Doctor of Philosophy

Discipline of Physiology

School of Molecular and Biomedical Sciences

Adelaide University

October 2008

3. PHENOTYPIC CHARACTERISATIONS OF TASTE CELLS OF THE MOUSE SMALL INTESTINE

3.1 Summary

Background: The alpha subunit of the taste G-protein gustducin, $G\alpha_{gust}$, is a key mediator of lingual sweet taste transduction and is additionally expressed in individual epithelial cells in the mouse intestine. $G\alpha_{gust}$-dependent signalling mechanisms may therefore be employed by epithelial chemosensory cells to trigger nutrient feedback from the small intestine. Potential primary chemoreceptive cell types include specialised epithelial brush cells that are suggested to release nitric oxide and enteroendocrine cells. 5-hydroxytryptamine (5-HT) and glucagon-like peptide-1 (GLP-1) contained in enteroendocrine cells are implicated in carbohydrate-stimulated gastrointestinal reflexes and behavioural responses however the transduction mechanisms that trigger their release from enteroendocrine cells are unknown. *Aims:* To determine which cell phenotypes may use $G\alpha_{gust}$-mediated transduction pathways in the mouse small intestine. *Methods:* Frozen sections from regions of the small intestine of perfusion-fixed adult male C57 mice were processed for indirect immunofluorescence histochemistry using $G\alpha_{gust}$ primary antibody. Additional sections were processed in combination with antibodies for 5-HT, GLP-1 and neuronal nitric oxide synthase (nNOS), and for the brush cell binding lectin, Ulex europaeus agglutinin (UEA-1). *Results:* Epithelial cells immunoreactive for $G\alpha_{gust}$ were present throughout the small intestine with peak expression in the jejunum. Here, $G\alpha_{gust}$ was expressed in subpopulations of epithelial cells that were colabelled with enteroendocrine cell markers 5-HT (27 ± 2%) or GLP-1 (15 ± 2%), or the brush cell marker UEA-1 (57 ± 4%). $G\alpha_{gust}$ cells that colabelled for 5-HT or GLP-1 showed distinct morphology and immunolabelling for $G\alpha_{gust}$ compared to those that colabelled with UEA-1. Immunolabelling for nNOS was absent from the epithelium despite strong labelling in the myenteric plexus. *Conclusions:* Subsets of enteroendocrine and

brush cells express $G\alpha_{gust}$ in the mouse jejunum. Intestinal nutrients may therefore be signalled by the release of 5-HT, GLP-1 from enteroendocrine cells or non-nitrergic mediators from brush cells. In addition, this data suggests 5-HT and GLP-1 may be released via both $G\alpha_{gust}$-dependent and independent pathways but $G\alpha_{gust}$-dependent release is likely to be confined to the jejunum.

3.2 Introduction

The ability of the intestinal mucosa to distinguish specific chemicals is evidenced in the many nutrient-evoked gastrointestinal reflexes which are initiated from the small intestine (77, 266, 267). The epithelial cell layer provides a barrier between ingested material and intestinal tissue and represents the key interface for chemical recognition. In response to the chemical composition of luminal contents specialised chemosensory cells in the epithelium release various neuroendocrine and endocrine mediators.

The molecular recognition of luminal carbohydrates occurs via an as yet unknown mechanism. It is now clear, however, that molecules that mediate sweet taste transduction in taste cells of the tongue also reside in the gastrointestinal mucosa, as described in Chapter Two. A taste-like molecular pathway is therefore a possible transduction mechanism triggered by luminal carbohydrates and may be present in one or more epithelial chemosensory cell types, such as enteroendocrine or brush cells.

Mediators released from enteroendocrine cells play an important role in the regulation of gastrointestinal functions and food intake through endocrine and neuroendocrine interactions (31) and unique profiles of enteroendocrine cell products are released in response to specific stimuli. Luminal carbohydrates in particular stimulate the release of gastric inhibitory polypeptide (GIP) (335), glucagon-like peptide 1 (GLP-1) (283, 324) and 5-HT (170, 204, 263). However we currently have little information about how such chemical signals in the lumen are perceived by enteroendocrine cells and the transduction mechanisms which lead to

their release. As a number of enteroendocrine mediators may be released in response to an individual nutrient, the chemosensory elements expressed in nutrient-sensing cells along the small intestine may vary. Indeed, the intestine may sense nutrient at multiple sites and recruit diverse and cascading sensing strategies depending on luminal concentration and the length of intestinal exposure (188, 193).

Brush cells, a specialised epithelial cell of the respiratory and gastrointestinal tracts, for over 10 years have been proposed to have a chemosensory function based on their morphological similarities to taste cells and their immunoreactivity for $G\alpha_{gust}$, the alpha-subunit of the taste G-protein complex key to taste transduction in lingual taste cells (92, 135, 137, 304). They can be characterised by the presence of a 'brush' or tuft of apical microvilli which extends into the lumen with long rootlets (279). In addition to structural differences, brush cells can be differentiated from surrounding enterocytes by the pattern of immunolabelling of cytoskeletal markers villin and cytokeratin 18 (CK18) (134) (although these proteins are present in enterocytes and other cell types and are therefore not exclusive markers), and in the mouse intestine, by the α-L-fucose binding lectin ulex europaeus agglutinin (UEA-1) (104). The proposed role of brush cells as chemoreceptors raises the question of how they could fulfil a signalling role when devoid of the secretory granules or transmitter vesicles that are a feature of enteroendocrine cells. However a study of brush cells in the rat gastric cardia and pancreatic duct revealed the presence of immunoreactivity for neuronal nitric oxide synthase (nNOS) (179) suggesting that brush cells may use nitric oxide (NO) as a gaseous messenger to signal to other structures within the gastrointestinal tract.

As illustrated in Chapter 2, the presence of $G\alpha_{gust}$ and other taste protein immunoreactivity in solitary cells of the intestinal epithelium suggests that that these cells possess a taste cell-like transduction pathway and are likely to be primary chemosensory cells for luminal nutrient feedback. However information on $G\alpha_{gust}$-expressing epithelial cell type(s) throughout the small intestine is lacking. In the original work which demonstrated $G\alpha_{gust}$-immunopositive cells in the rat duodenum, Höfer and colleagues (137) showed that

expression was confined to brush cells. The lack of $G\alpha_{gust}$-immunolabelling in cells immunoreactive for the general enteroendocrine cell marker chromogranin A (CgA) or for 5-HT suggested that $G\alpha_{gust}$ was not expressed in duodenal enteroendocrine cells. However this study did not assess other enteroendocrine cells subtypes – this is of direct relevance as CgA may not represent the major chromogranin subtype present in all enteroendocrine cells (40). This is particularly true in the mouse small intestine, where it has been reported that enteroendocrine cells that produce GIP, GLP-1 and cholesystokinin contain little if any CgA (357). Consequently it is possible that $G\alpha_{gust}$ may be more widely expressed in mouse intestinal enteroendocrine cells than first suggested. Indeed, transcript for $G\alpha_{gust}$ has been identified in the enteroendocrine cell line STC-1 using RT-PCR (366) whereas it was not present in an enterocyte cell line (81).

In terms of intestinal carbohydrate feedback modulation of gastric motility, two enteroendocrine cell products are of particular interest. 5-HT released from enterochromaffin cells and GLP-1 from L cells are both implicated in the vagal mechanism of delayed gastric emptying (155, 269). Enteroendocrine cell subtypes have distinct regional distributions throughout the gut (282) as their specific actions are required at various points in the digestive process. Expression of chemosensory transduction molecules, such as $G\alpha_{gust}$, in these enteroendocrine cell types in small intestinal regions relevant to feedback initiation may provide clues to the transduction mechanisms involved in carbohydrate-evoked release of 5-HT and GLP-1.

The aim of these studies, therefore, was to quantify the regional expression of $G\alpha_{gust}$ in the mouse small intestine, and to identify the phenotype of 'taste' cells and their potential signalling mediators. This information will indicate which cells are equipped to use $G\alpha_{gust}$-dependent signalling pathways and may provide important information on their role in gastrointestinal function. In this case double label immunohistochemistry was used to assess colocalisation of $G\alpha_{gust}$ with markers of enteroendocrine cells of interest and brush cells.

3.3 Aims

1. To quantify $G\alpha_{gust}$ immunopositive cells throughout the mouse small intestine.

2. To determine if $G\alpha_{gust}$-dependent signalling mechanisms are present in small intestinal epithelial cells equipped to release 5-HT, GLP-1 or NO.

3.4 Specific hypotheses

1. $G\alpha_{gust}$ is expressed in individual epithelial cells throughout the mouse small intestine with longitudinal and radial expression patterns consistent with a role in chemosensation.

2. $G\alpha_{gust}$ is expressed in small intestinal brush cells in mouse, which can be identified by binding of lectin UEA-1 and which co-express nNOS.

3. $G\alpha_{gust}$ is expressed in small intestinal enteroendocrine cells in mouse, which can be identified by immunolabelling for 5-HT or GLP-1.

3.5 Materials and methods

All experiments were performed using adult male C57BL/6 mice aged 7-10 weeks, housed conventionally with free access to water and a standard laboratory rodent diet. All studies were performed in accordance with the Australian code of practice for the care and use of animals for scientific purposes and with the approval of the Animal Ethics Committees of the Institute of Medical & Veterinary Science (Adelaide,

Australia) and the University of Adelaide.

3.5.1 Animal and tissue preparation

Animals and tissues were prepared as detailed in the methods section of Chapter Two. Briefly, adult male C57BL/6 mice were anesthetised by 0.1mL sodium pentobarbitone (60mg/kg) i.p. and transcardially perfused with warm heparinised saline followed by cold 4% paraformaldehyde in 0.1M phosphate buffered saline (PBS), pH 7.4. After fixation the entire length of the small intestine was removed, opened longitudinally along the cephalocaudal axis, pinned flat and flushed with fresh fixative and left to post-fix in paraformaldehyde-PBS for 2-4 hrs at room temperature. The tissue was subsequently washed three times in PBS than cryoprotected in 30% sucrose/PBS overnight at 4ºC. The entire small intestine from pylorus to caecum was sectioned into 1.5cm blocks and embedded in cryomoulds in O.C.T compound (Tissue-Tek) and rapidly frozen in liquid nitrogen. Frozen blocks of intestinal segments were designated as duodenum, proximal jejunum, mid jejunum, distal jejunum and ileum as indicated in Figure 3.5.1. These regional definitions were based on distance from the pylorus with the average length of the fixed small intestine measuring approximately 30 cm. Starting from the pylorus the duodenum was defined as the intestinal segments within 0-4 cm, proximal jejunum as 6-10 cm, mid jejunum; 12-16 cm, distal jejunum; 18-22 cm and ileum 24-30 cm. Frozen sections from each defined region were cut at 14µm on a cryostat (CRYOCUT 1800 Reichert-Jung) and thaw mounted directly onto gelatine coated glass slides.

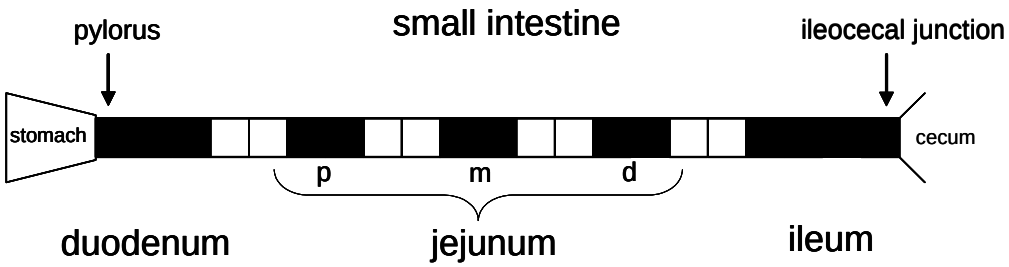

Figure 3.5.1 Regional classifications of mouse small intestine segments.
After fixation, the entire length of the mouse small intestine from the pylorus to ileocecal junction was divided and frozen in 1.5cm blocks. Based on their location along the longitudinal axis these intestinal segments were defined as belonging to the duodenum, proximal (p) jejunum, mid (m) jejunum, distal (d) jejunum or ileum. Sections designated as belonging to these regions were obtained from blocks in the shaded areas within the boundaries of the classified region.

3.5.2 Single label immunohistochemistry

Immunoreactivity for $G\alpha_{gust}$ was detected using the rabbit polyclonal anti-$G\alpha_{gust}$ antibody and indirect immunofluorescence protocol detailed in chapter two. This protocol was also followed for detection of nNOS immunoreactivity. Alternate assays for nNOS immunoreactivity were performed using two different rabbit polyclonal antibodies (AB1552, Chemicon-Millipore, Boronia, Australia, working dilution 1:200 and 61-7000, Zymed Laboratories, working dilution 1:500).

3.5.3 Double label immunohistochemistry

A double-label indirect immunofluorescence protocol for simultaneous detection of $G\alpha_{gust}$ and 5-HT or GLP-1 immunoreactivity was performed in single small intestinal sections by using primary antibodies raised in different species. Immunoreactivity for 5-HT was detected using a mouse monoclonal antibody (Clone 5-HT-H209, M0758, DakoCytomation, Glopstrup, Denmark, working dilution 1:100). GLP-1 immunoreactivity was detected by a goat polyclonal antibody (SC7782, Santa Cruz Biotechnology, working dilution 1:100). Primary antibodies were visualised by detection with alternate Alexa Fluor conjugated secondary antibodies (1:200, Invitrogen, Mount Waverly, Australia). The primary antibody working dilutions for 5-HT and GLP-1 were determined in preliminary assays using a range of dilutions to find the best immunofluorescence signal while providing low background labelling. No labelling of 5-HT or GLP-1 in epithelial cells occurred in negative control sections.

The sections were first processed using the rabbit polyclonal $G\alpha_{gust}$ antibody single-label immunohistochemical protocol detailed in Chapter 2. Following the anti-rabbit secondary antibody incubation a sequential single label protocol was commenced by performing an additional blocking step for 1 hr at room temperature. This was followed by an overnight incubation at 4°C with either 5-HT or GLP-1

primary antibody. Sections were then washed in PBS-T and subsequently incubated for 1 hr at room temperature with a species-specific secondary antibody of an alternate fluorophore colour to that binding the $G\alpha_{gust}$ primary antibody. Sections were washed finally in PBS-T and mounted in ProLong Antifade reagent (Invitrogen) and coverslipped. Negative controls where one and both primary antibodies were omitted were performed in each assay run.

3.5.4 Lectin histochemistry

The L-fucose residue binding lectin, Ulex europaeus agglutinin-1 (UEA-1), was used in biotinylated form (B-1065, Vector Laboratories, Burlingame, CA) as a surrogate marker of intestinal brush cells in mice. Sections were air dried for 10 – 15 mins at RT then washed three times for 10 mins with PBS-T. Sections were incubated with biotinylated UEA-1 in a 1:500 dilution with PBS-T for 2-3 hours at RT. Unbound UEA-1 was removed by three washes of PBS-T before sections were incubated with streptavidin Alexa Fluor 350 conjugate (S11249, Invitrogen, 1:200 in PBS-T) for 1 hour at RT. Sections were washed again in PBS-T and then immediately underwent either the $G\alpha_{gust}$ single or double label immunohistochemical protocols described above.

Preliminary assays were run to determine the optimal working dilution of biotinylated UEA-1. Additional sections were assayed omitting the biotinylated UEA-1 or streptavidin Alexa Fluor 350 or both to create negative controls and in these sections no labelling of epithelial cells was observed.

3.5.5 Visualisation and quantification

Sections were examined and images obtained on an epifluorescence microscope (BX-51,Olympus) equipped with multiple excitation filters. Images were acquired on a monochrome charge-coupled device

digital camera system (Photometrics CoolSNAP*fx*, Roper Scientific, Tuscon AZ). Fluorescence images were imported unmodified into V^{++} Precision Digital Imaging System software (version 4.0, Digital Optics, Auckland, New Zealand), pseudo-coloured and merged for composite images.

The number of epithelial cells immunopositive for $G\alpha_{gust}$ in each transverse section of intestine were manually counted at the microscope, according to published methods (290). The number of immunopositive cells were then averaged over a minimum of 50 sections representative of each defined intestinal segment from 4-6 mice. Differences in the number of immunopositive $G\alpha_{gust}$ cells between small intestinal regions were assessed using a one-way ANOVA with Tukey's multiple comparison tests (Prism 3.02; Graphpad, San Diego, CA). A p value of < 0.05 was considered significant and results were expressed as mean ± SEM.

In double-labelled sections from mouse jejunum $G\alpha_{gust}$ immunopositive cells were identified and counted prior to visualisation of co-labelling for 5-HT, GLP-1 or UEA-1 under the relevant secondary antibody filter. $G\alpha_{gust}$ immunopositive epithelial cells colabelled for 5-HT, GLP-1 or UEA-1 were represented as a proportion of the total number of $G\alpha_{gust}$ immunopositive averaged from pooled counts of a minimum of 10 sections (range 10-40) per assay from each of four mice.

3.6 Results

Characterisation of $G\alpha_{gust}$ immunopositive cells and their distribution in the small intestine

As reported (Chapter 2), $G\alpha_{gust}$ immunoreactivity in the small intestine was specifically located in solitary cells within the villous epithelium. Immunolabeled cells were all of open cell type in that their apical tip extended to the brush border membrane and had direct access to the lumen. Immunoreactivity for $G\alpha_{gust}$ in

each cell was homogenous throughout the cytoplasm but was prominent at the apical tip of the cell and in the brush border (Figure 3.6.1).

$G\alpha_{gust}$-immunoreactive cells in the epithelium of the small intestine occupied a preferential location within the crypt-villus axis, with the majority of cells located at the upper villus and close to the villi tip (Figure 3.6.2). $G\alpha_{gust}$-immunoreactive cells were also identified at lower abundance in the mid-regions along the villi length within the jejunum (Figure 3.6.3). However $G\alpha_{gust}$-immunopositive cells were only occasionally found in the epithelium of the lower villus or crypts (Figure 3.6.4).

The number of $G\alpha_{gust}$-immunopositive cells in the intestinal villi also varied according to region (Figure 3.6.5). Immunopositive cells were rare in duodenal sections (0.5 ± 0.1) cells/section, range 0-2 cells/section), were routinely found in the proximal jejunum (1.3 ± 0.2 cells/section, range 0-5 cells/section) and reached peak frequency at the mid jejunum (7.5 ± 0.7 cells/section, range 0-25 cells/section). $G\alpha_{gust}$ immunoreactive cells decreased in frequency beyond the mid jejunum in sections from the distal jejunum (2.1 ± 0.3 cells/section, range 0-9 cells/section) and ileum (3.0 ± 0.3 cells/section, range 0-10 cells/section). Sections from the mid jejunum region contained the highest number of $G\alpha_{gust}$-immunopositive epithelial cells compared to all other small intestine regions ($p < 0.05$) (Figure 3.6.6). Although $G\alpha_{gust}$-immunoreactive cells were present throughout the distal small intestine, those in the ileum had a distinctly different cell shape (Figure 3.6.7), and were more ovoid in shape with a broader apical region. In some preliminary survey sections, $G\alpha_{gust}$-immunoreactive cells were also found to be scattered throughout the colonic epithelium, in a similar manner to those in small intestinal regions (Figure 3.6.8). Despite the fact that this colonic $G\alpha_{gust}$ cell population was not quantified they appeared to be present at lower abundance than in the small intestine. No further investigations of colonic $G\alpha_{gust}$-immunoreactive cells were undertaken in these studies.

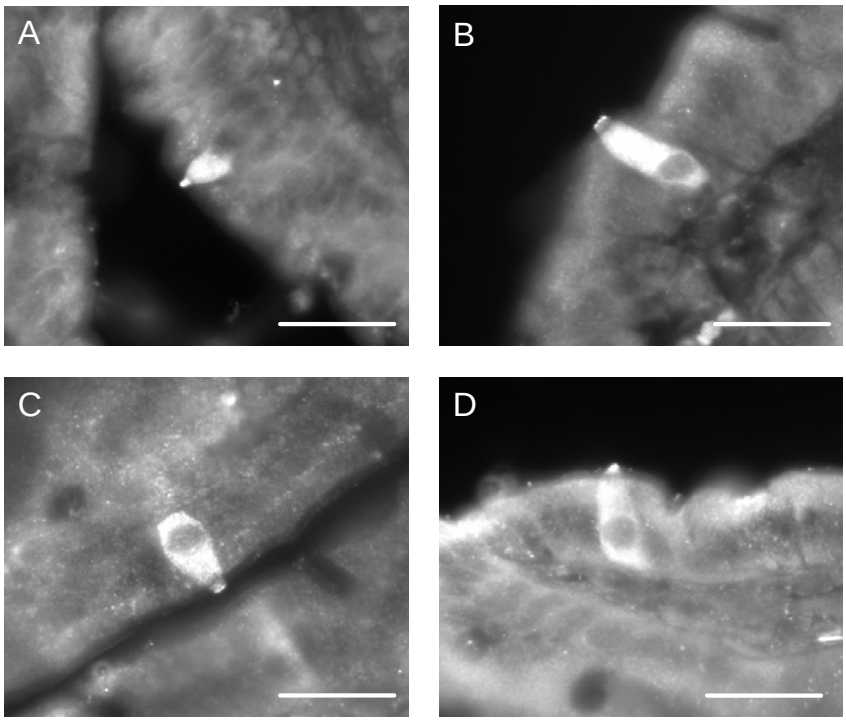

Figure 3.6.1 Brush border membrane immunoreactivity in Gα_{gust}-positive cells in the villous epithelium.
Typically immunolabelling with primary antibody for Gα_{gust} in the mouse small intestine results in strong immunoreactivity throughout the cytoplasm of individual epithelial cells. In sections where the apical tip of immunopositive cells is visible strong immunoreactivity is also clearly observable in the brush border membrane (A-D). Scale bars = 50µm.

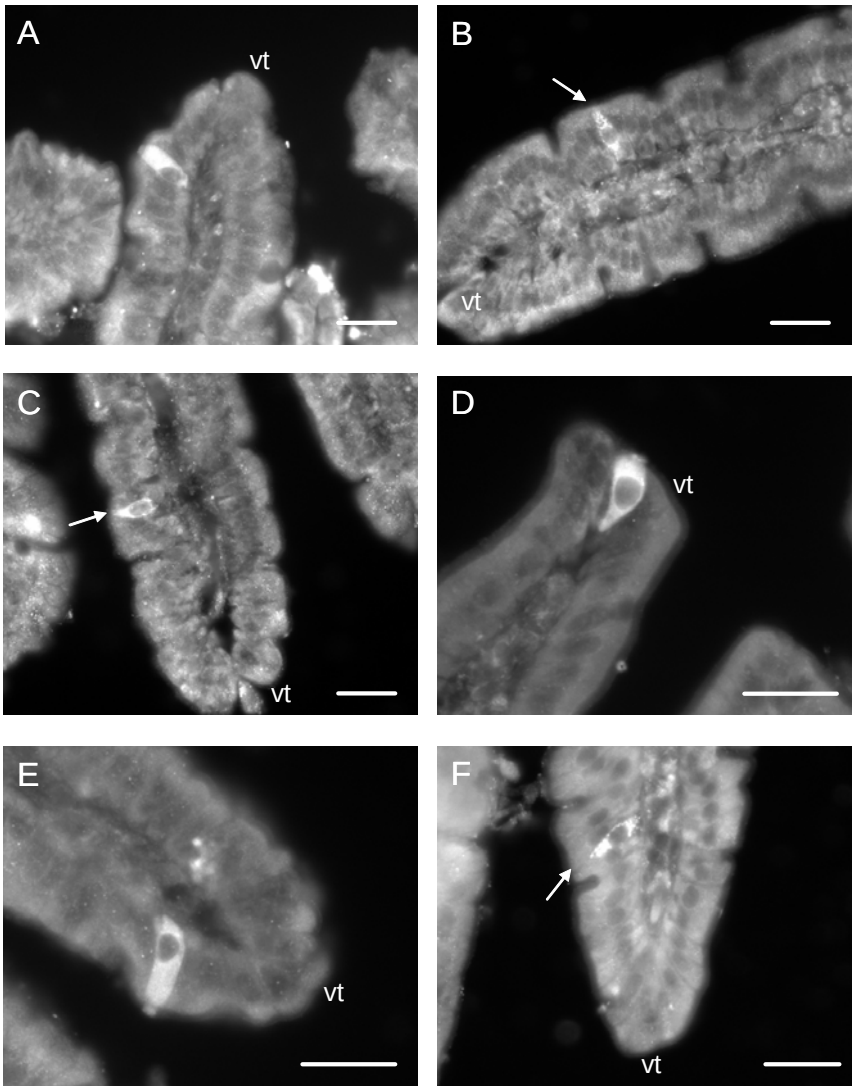

Figure 3.6.2 Gα_{gust} immunoreactive cells are most frequently associated with the upper villus and villus tip.

The location of Gα_{gust} immunopositive cells in the surface epithelium of the intestinal villi appears to display some regional specificity along the crypt-villus axis. Positive cells are most frequently observed in the upper villus (A-F). Within the upper regions of the villi, immunopositive cells are often found located at or very close to the villi tip (vt) (A, D, E). Scale bars = 50µm.

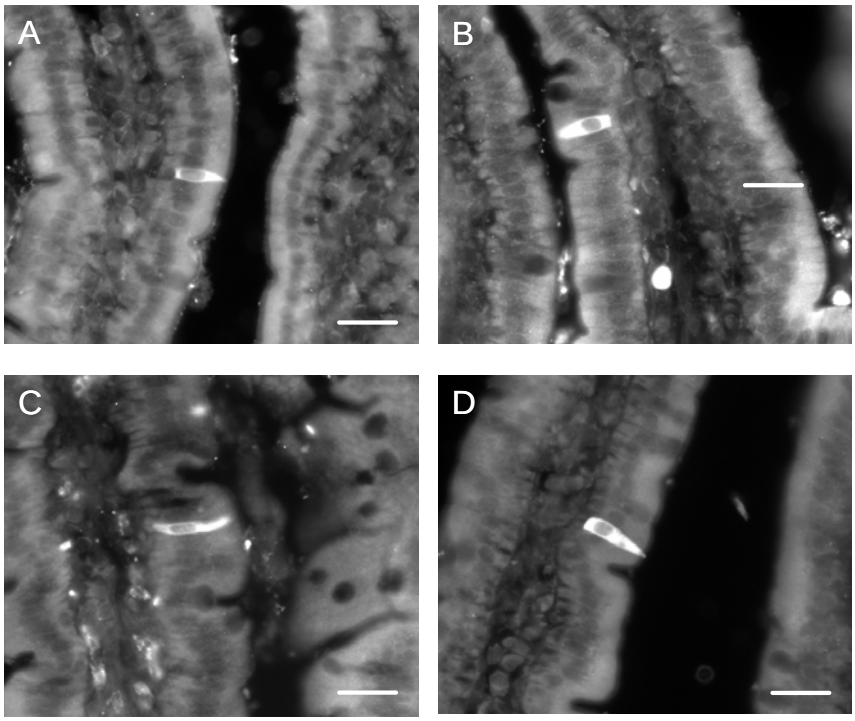

Figure 3.6.3 Gα_{gust} immunoreactivity in cells located along the mid crypt-villus axis in jejunal villi. Gα_{gust} immunoreactive cells in the mouse small intestine were most frequently located at or near the villus tip, however they were also observed in the mid regions of individual villi. Gα_{gust} immunopositive cells in the epithelium of the mid villus are shown (A-D) in sections from the jejunum. Scale bars = 50µm.

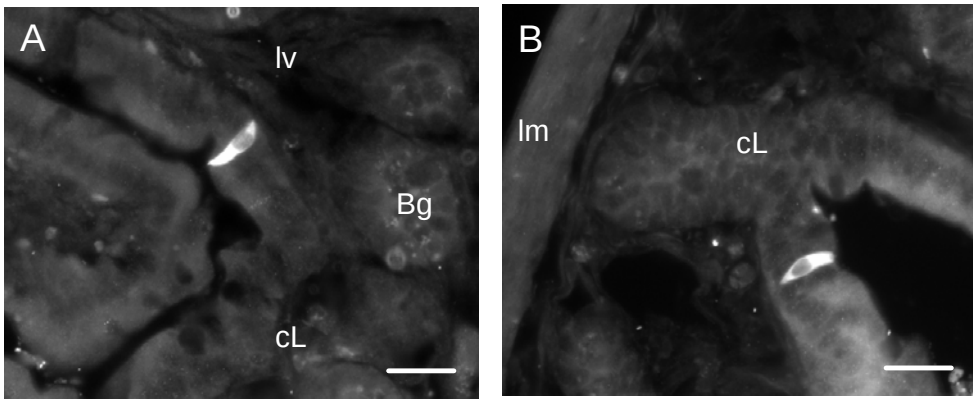

Figure 3.6.4 Rare Gα_{gust} immunoreactive cells in the villus crypts in mouse small intestine.
In the mouse small intestine, cells immunopositive for Gα_{gust} are preferentially located in the epithelium near the villus tip. Immunoreactive cells were only rarely observed in the epithelium towards the lower villi (lv) and crypts of Lieberkühn (cL) or in the glandular epithelium (Bg; Brunner's gland). These Gα_{gust} immunopositive cells shown in the lower villous epithelium near the cryptal region (A-B) are rare examples. lm; longitudinal muscle layer. Scale bars = 50µm.

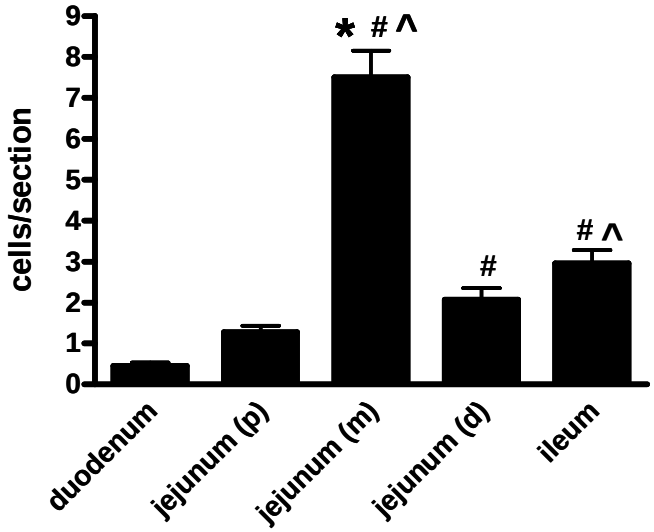

Figure 3.6.5 Regional specificity in frequency of Gα_{gust} immunopositive cells in the small intestine. The number of Gα_{gust} immunoreactive cells per sections varied with region of the small intestine. Average Gα_{gust}-positive cell count per section is shown for each intestinal region (Mean ± SEM, N = 6). Gα_{gust}-immunopositive cells were preferentially located in the mid jejunum. *Significantly different from all other intestinal regions (one-way ANOVA; $p < 0.001$). #Significantly different from duodenum ($p < 0.05$). ^Significantly different from proximal jejunum ($p < 0.01$). p; proximal, m; mid, d; distal.

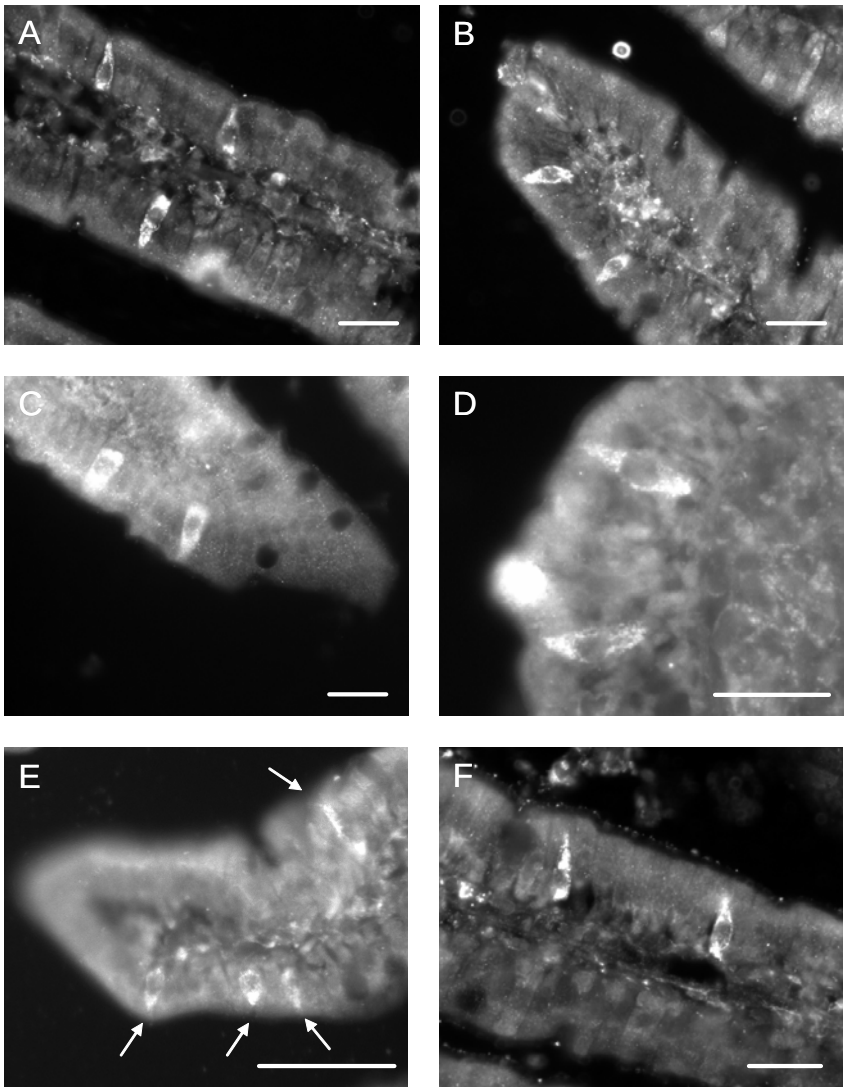

Figure 3.6.6 Gα_{gust} immunopositive cells were most abundant in the jejunum.
Intestinal sections from the mid jejunum region contain more G_{gust} immunoreactive cells compared to all other regions of the mouse small intestine. This higher frequency of immunopositive cells in this region can clearly be seen in sections from the jejunum where examples of two (B,C,D,F) or more (A, E) Gα_{gust}-immunoreactive cells can be seen in close proximity within the epithelium of individual villi. Four immunoreactive cells (arrows) are found in a single villus, closely associated with the villus tip. NB: Labelling seen within the lamina propria is not specific to the primary antibody and appears to be immunofluorescing immune cells which are observable on negative controls.
Scale bars = 50µm.

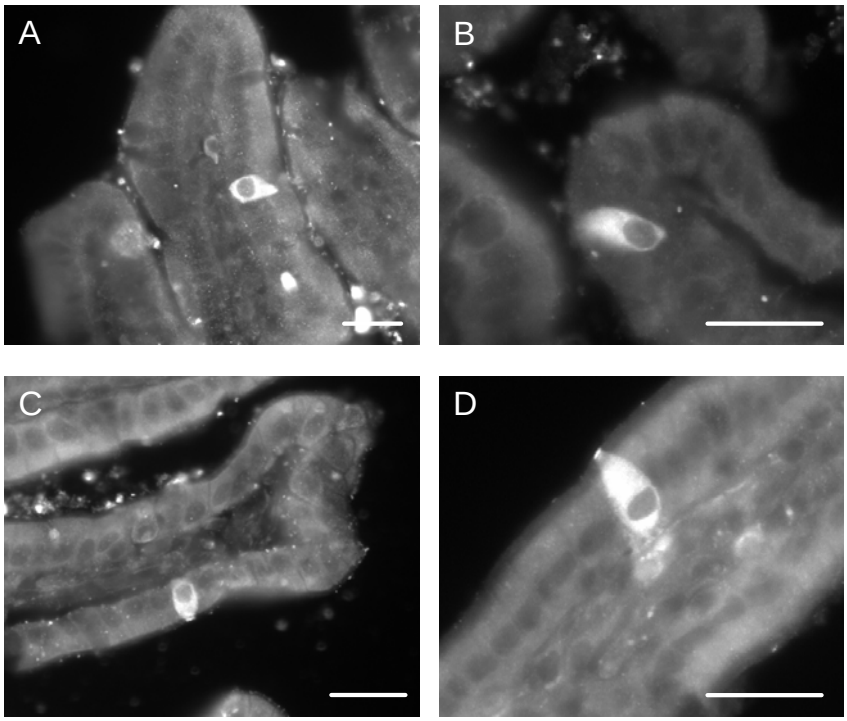

Figure 3.6.7 Characteristic appearance of Gα_{gust} immunoreactive cells in the ileum.
Gα_{gust} immunoreactive cells in sections from the ileum appeared to visually differ from those in the more proximal regions of the small intestine. These cells displayed a solid pattern of strong immunoreactivity across the cytoplasm and were notably more ovoid in shape with a broader apical process than proximal immunoreactive cells (A-D). Scale bars = 50μm.

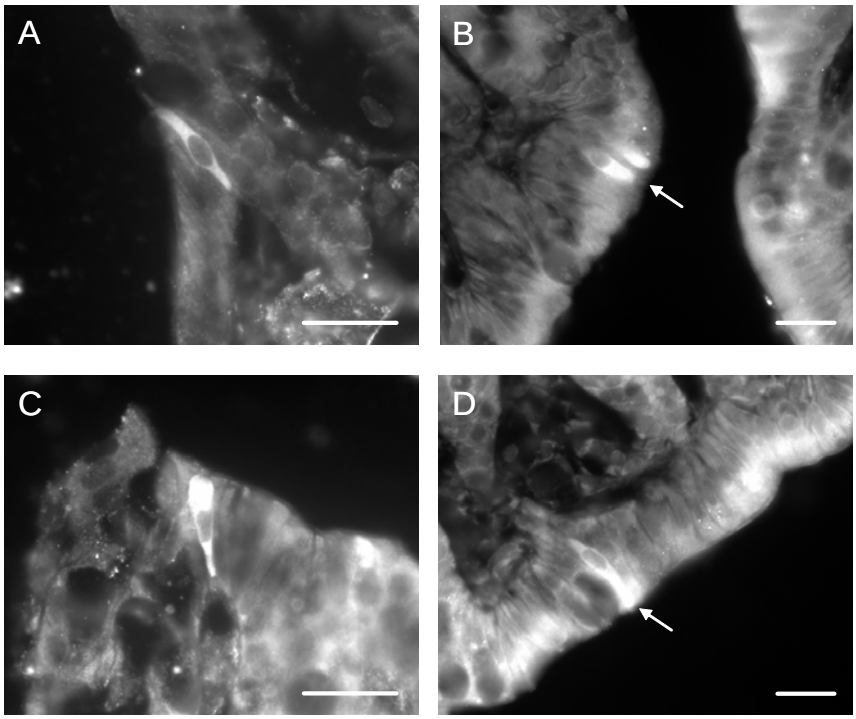

Figure 3.6.8 Gα_{gust} immunoreactivity in individual cells of the colonic epithelium.
Preliminary survey sections of the mouse colon processed with Gα_{gust} primary antibody revealed immunolabel within individual cells in the epithelium (A-D). Colonic Gα_{gust} immunoreactive cells appeared to be located in the surface epithelium of the colon and be of the open cell type as to have access to the lumen. Scale bars = 50µm.

$G\alpha_{gust}$-positive cells and 5-HT immunoreactivity in the small intestine

Immunoreactivity for 5-HT in the villous surface and glandular epithelium of the small intestine was evident within singly dispersed cells throughout the entire length of the small intestine and was detected throughout the cytoplasm but most commonly found concentrated in the basolateral portion of the cells. 5-HT immunoreactive cells in the villous epithelium were present in larger numbers than $G\alpha_{gust}$ immunoreactive cells. In dual labelling assays for $G\alpha_{gust}$ and 5-HT it was apparent that immunoreactivity for both was predominantly contained within separate populations of solitary epithelial cells (Figure 3.6.9). Indeed, in the distal regions of the small intestine no epithelial cells co-expressed 5-HT and $G\alpha_{gust}$. However, in the mid jejunum, where the highest abundance of $G\alpha_{gust}$ expressing cells were located a subset of $G\alpha_{gust}$ expressing cells also contained immunoreactivity for 5-HT (27 ± 2%, n = 4, Figure 3.6.10). Within these co-labelled cells patterns of labelling for each antigen were distinct with $G\alpha_{gust}$ expressed throughout the cell with peak abundance in the apical region, while 5-HT was predominantly compartmentalised in the basolateral region of the cell.

Labelling with the $G\alpha_{gust}$ primary antibody produced the highest quality and consistency of immunolabelling in mouse small intestine compared to other taste molecule antibodies used in localisation studies (Chapter 2). As a consequence, the $G\alpha_{gust}$ antibody was used as the sole marker for further investigation of intestinal taste cell phenotypes. Despite this, preliminary double-label assays performed in the jejunum with antibodies to 5-HT and either T1R3 or $G\gamma_{13}$ showed similar proportions of cells colabelled for 5-HT and T1R3 or $G\gamma_{13}$ as those labelled with 5-HT and $G\alpha_{gust}$ (Figure 3.6.11).

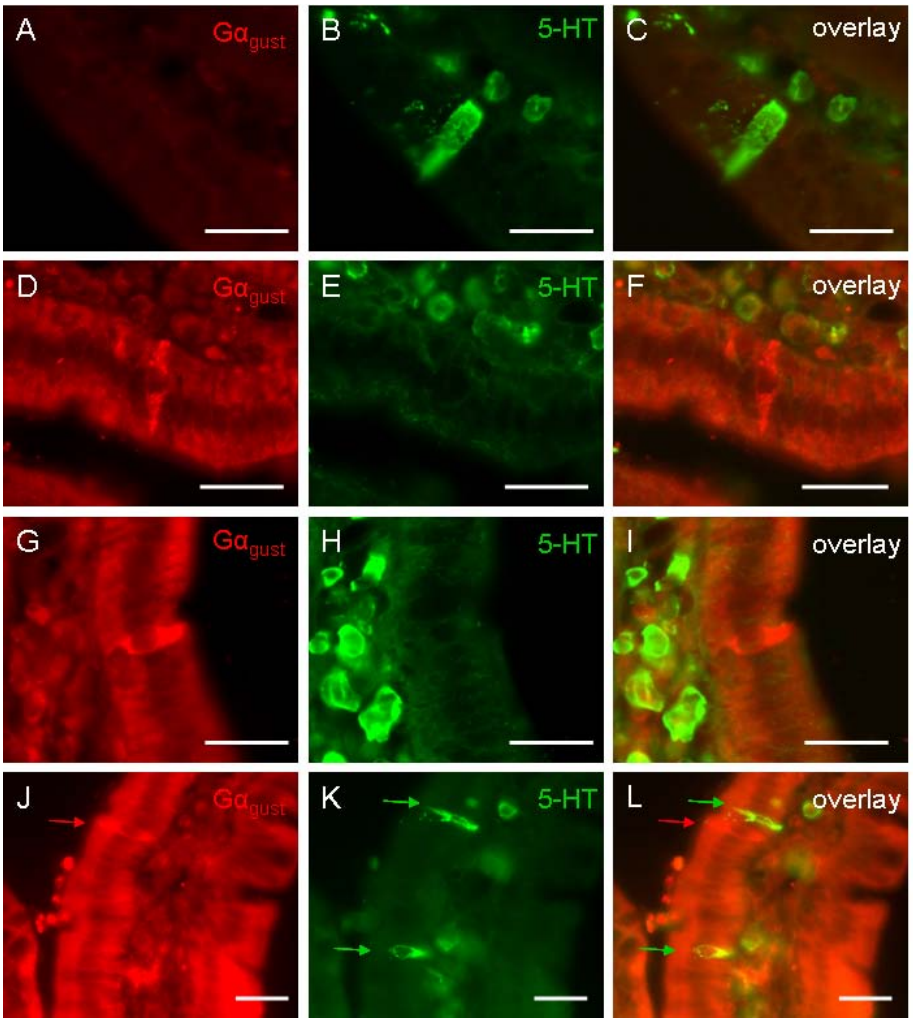

Figure 3.6.9 Gα_{gust} and 5-HT were expressed in separate cell populations in the mouse small intestine.

In double-label assays for Gα_{gust} and 5-HT, co-expression was not apparent in the majority of cells labelled by either primary antibody. A 5-HT immunopositive cell (green fluorescence B) contains no immunoreactivity for Gα_{gust} (A) confirmed in the composite image (C). Gα_{gust} immunopositive cells (red fluorescence D and G) similarly were devoid of 5-HT immunoreactivity (E and H) clearly shown by only red fluorescence in the cells in the composite image (F and I). Within the same region of epithelium within a single villi, an Gα_{gust} immunopositive cell (red arrow, J) and two 5-HT immunopositive cells (green arrow, K) are evident. In the composite image (L) Gα_{gust} and 5-HT immunoreactivities are clearly contained within different cells (arrows). NB: 5-HT also labels mast cells in the lamina propria. Scale bars = 50µm.

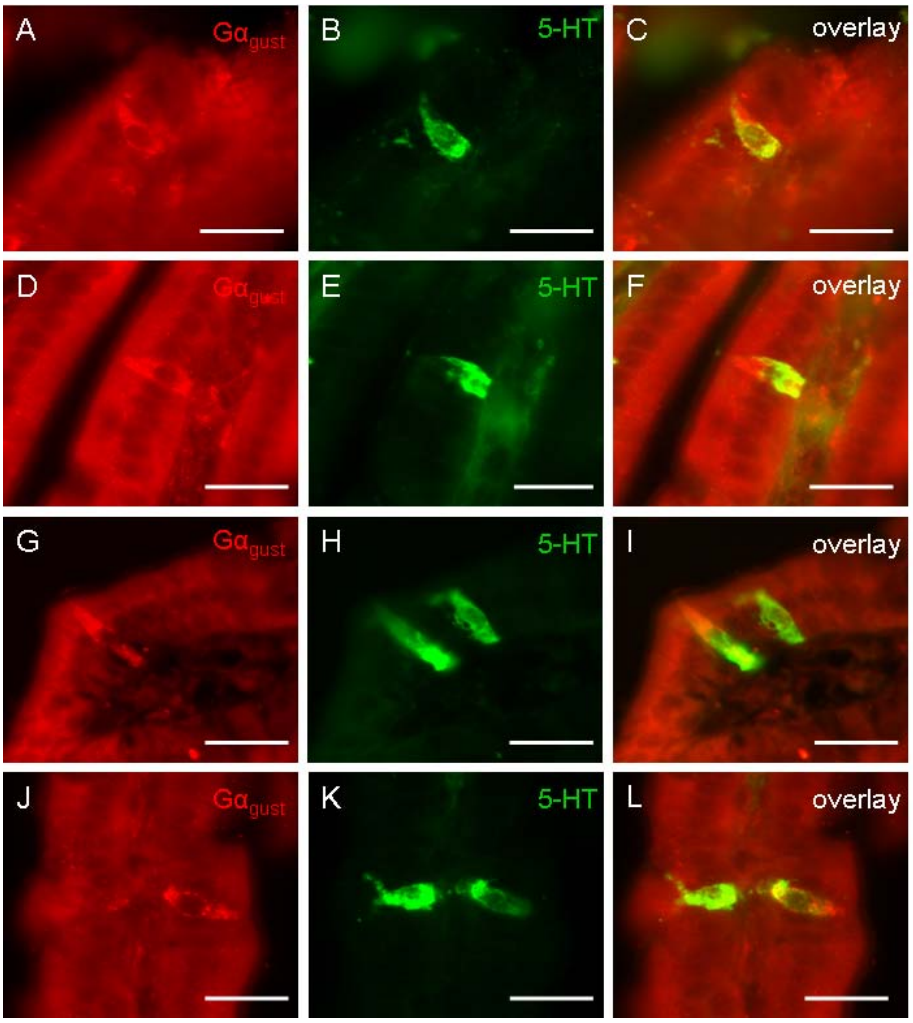

Figure 3.6.10 Gα_{gust} and 5-HT are coexpressed in a subpopulation of cells in the mouse jejunum. A subset of Gα_{gust} immunopositive cells (27 ± 2%, n = 4) in the mid jejunum were colabelled for 5-HT. An Gα_{gust}-postive cell (red fluorescence, A) shows 5-HT immunoreactivity (green fluorescence, B). A composite image (yellow, C) confirms localisation within the same cell. Within colabelled cells patterns of immunolabel for Gα_{gust} and 5-HT were often distinct, Gα_{gust} immunoreactivity (D) is apparent throughout the cytoplasm whereas 5-HT immunoreactivity (E) is often notably concentrated in the basolateral half of the cell. Composite image, F. A 5-HT-positive cell not colabeled with Gα_{gust} is shown in close proximity to a colabelled cell (I and L). Scale bars = 50µm.

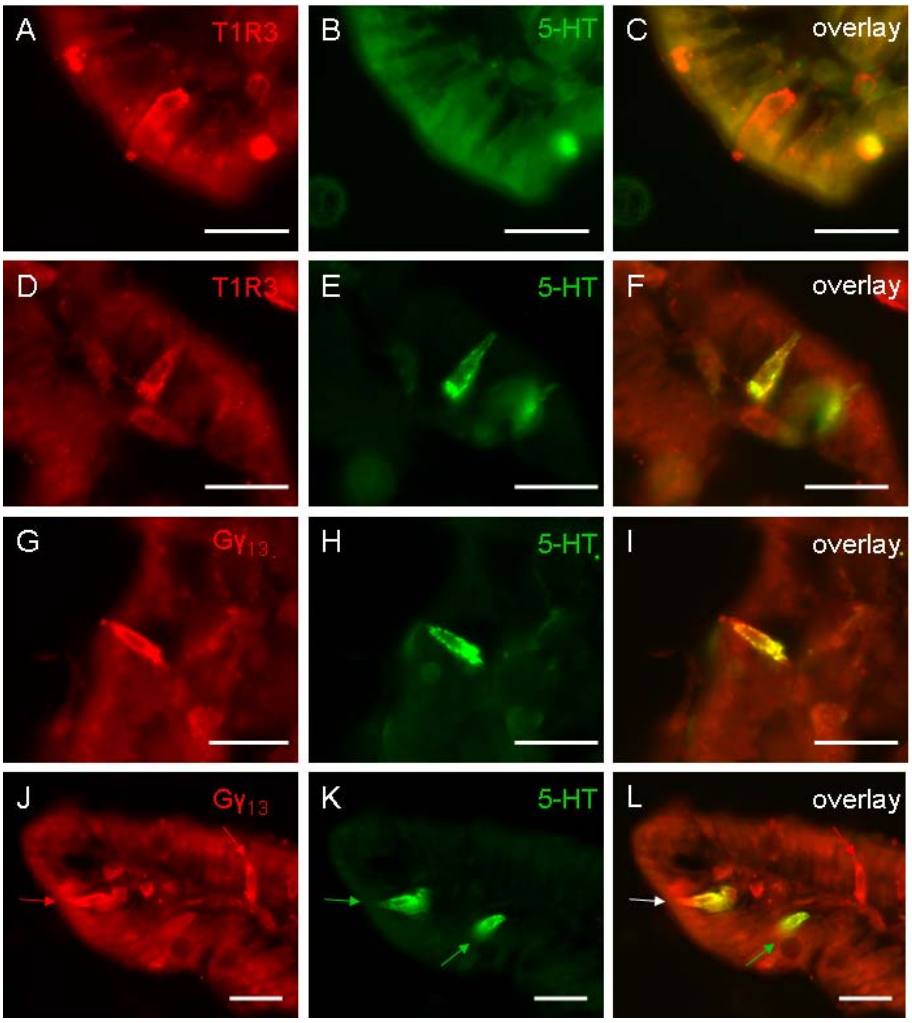

Figure 3.6.11 Coexpression of T1R3 and $G\gamma_{13}$ with 5-HT in mouse jejunum.
Preliminary double-label assays with 5-HT and T1R3 or $G\gamma_{13}$ indicate similar coexpression patterns as in assays with $G\alpha_{gust}$. T1R3 immunopositive cells (red fluorescence, A) appear immunonegative for 5-HT (B), composite image, C. A portion of T1R3-positve cells (red fluorescence, D) contain 5-HT immunoreactivity (green fluorescence, E) as confirmed in the composite image (yellow fluorescence, F). Similarly a $G\gamma_{13}$ immunoreactive cell (red fluorescence, G) is also immunopositive for 5-HT (green fluorescence, H), composite image, I. $G\gamma_{13}$ (red arrows, J) and 5-HT (green arrows, K) immunoreactivities in the epithelium are singly and co-expressed (L). Scale bars = 50µm.

$G\alpha_{gust}$-positive cells and GLP-1 immunoreactivity in the small intestine

GLP-1 immunoreactivity in the small intestine was contained within solitary cells in the villous and glandular epithelium. Like 5-HT positive cells, immunofluorescence for GLP-1 was concentrated in the basolateral portion of the cell. GLP-1 immunoreactive cells were a smaller population than those expressing 5-HT and were more common in the epithelium of the submucosal glands than in the villi, and more numerous in the distal portions of the small intestine. Throughout the small intestine immunolabelling for GLP-1 and $G\alpha_{gust}$ generally did not colocalise within the same cells (Figure 3.6.12). This was particularly true within the distal portions of the small intestine, where $G\alpha_{gust}$ and GLP-1 were present within separate cells that were found in different locations - with $G\alpha_{gust}$-positive cells concentrated in the upper villi while GLP-1-postive cells were predominantly found in the glandular epithelium. However, in the mid jejunum a small population of $G\alpha_{gust}$-positive cells co-expressed GLP-1 (15 ± 2%, n =4, Figure 3.6.13) which labelled in a pattern similar to that seen with 5-HT.

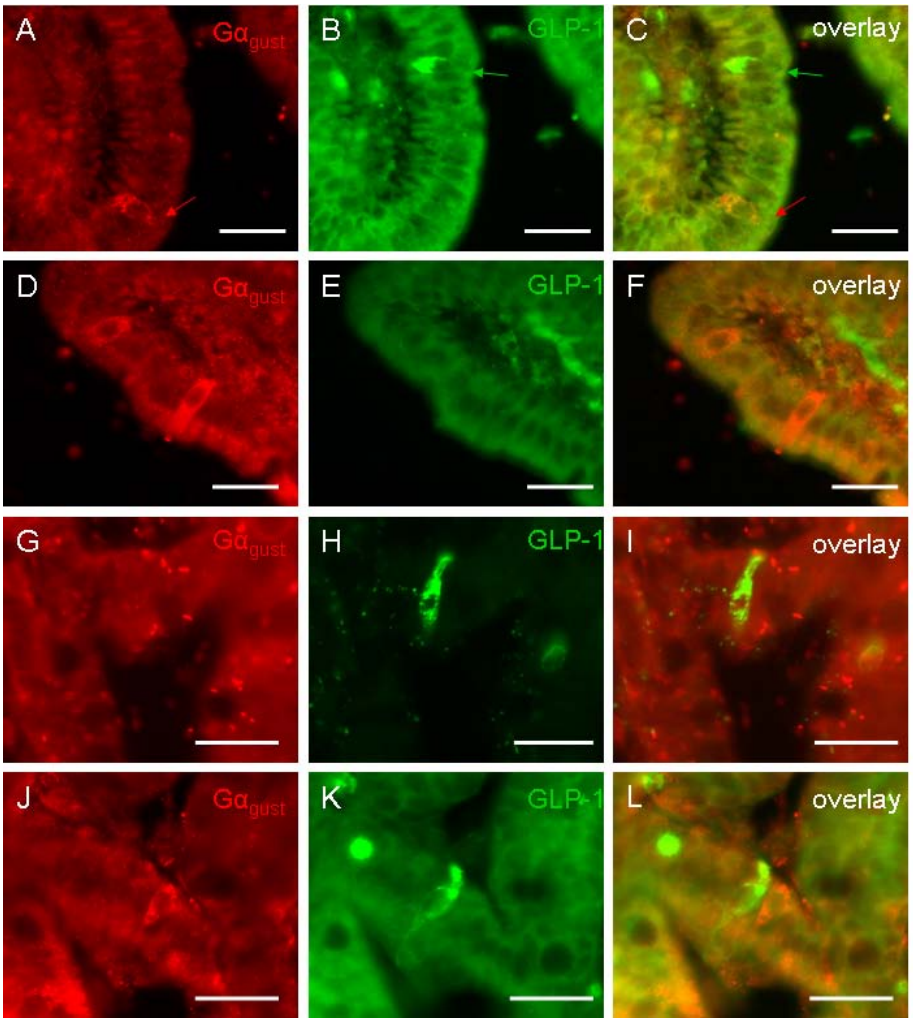

Figure 3.6.12 Gα_{gust} and GLP-1 were expressed in separate cell populations throughout the mouse small intestine.

Gα_{gust} (red arrow, A) and GLP-1 immunoreactivity (green arrow, B) are clearly contained within separate epithelial cells (composite image,C). Gα_{gust}-positive cells (red fluorescence, A) in the epithelium clearly contain no immunoreactivity for GLP-1 (green fluorescence, E), composite image, F. Similarly a GLP-1 positive cell (H) in the crypt region contains no immunoreactivity for Gα_{gust} (composite image, I). A rare Gα_{gust}-positive cell in the crypt region (red fluorescence, J) is located adjacent to a GLP-1-positive cell (green fluorescence, K). The composite image (L) confirms that although in close proximity immunolabelling for each antigen is contained within distinct cells. Scale bars = 50µm.

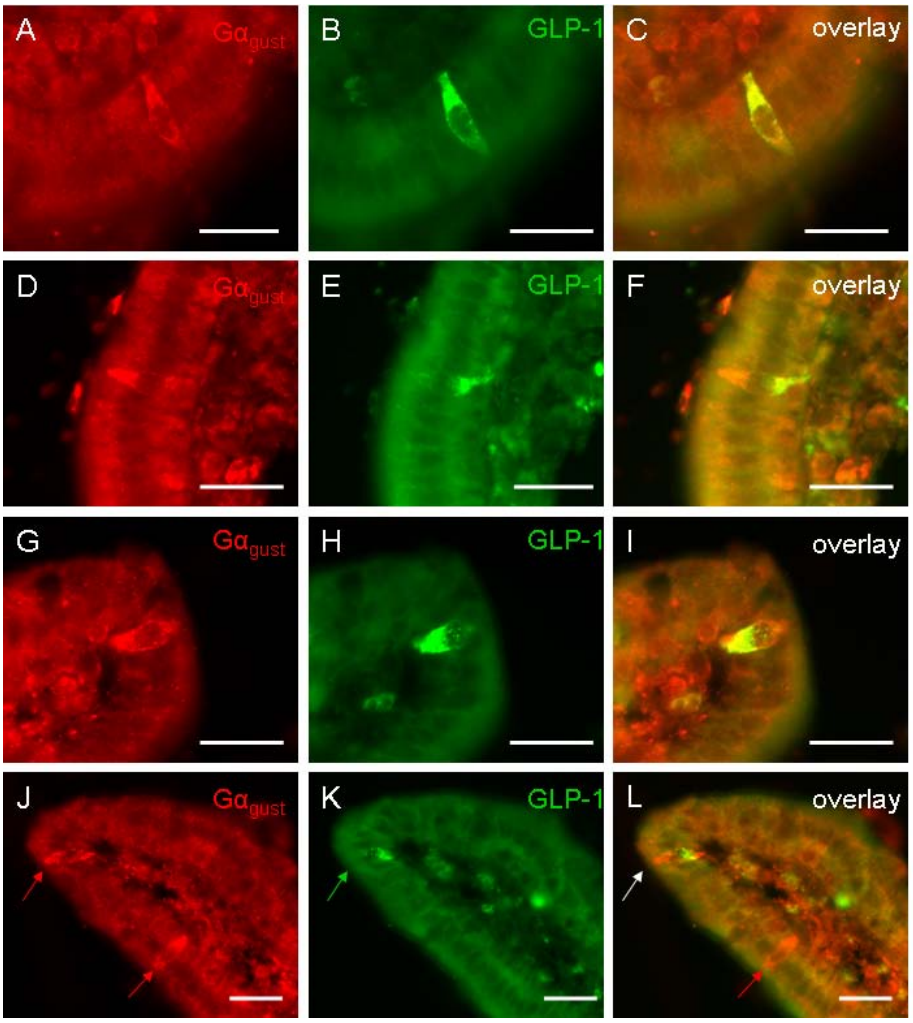

Figure 3.6.13 G**α**$_{gust}$ and GLP-1 were coexpressed in a subpopulation of cells in the mouse jejunum. A subset of Gα_{gust} immunopositive cells (15 ± 2%, n = 4) in the mid jejunum display colabel for GLP-1. An Gα_{gust}-postive cell (red fluorescence, A) contains GLP-1 immunoreactivity (green fluorescence, B). A composite image (yellow, C) confirms localisation within the same cell. Within colabelled cells patterns of immunolabel for Gα_{gust} and GLP-1 were often distinct, Gα_{gust} immunoreactivity (D and G) is apparent throughout the cytoplasm whereas GLP-1 immunoreactivity (E and H) is often notably concentrated in the basolateral half of the cell (composite images, F and I). Two Gα_{gust}-positive can be identified (red arrows, J) within the epithelium of the upper villi, however only one contains GLP-1 immunoreactivity (green arrow, K), illustrating the different subtypes of Gα_{gust}-positive cells in the region (composite, L). Scale bars = 50µm.

$G\alpha_{gust}$-positive cells and lectin UEA-1 label in the small intestine

UEA-1 labelling was widespread throughout the small intestine, where it was evident in individual epithelial cells. UEA-1 label was evident throughout the cytoplasm in labelled cells but was more commonly restricted to the apical portion of the cell, indicating strong binding to the glycocalyx. The majority of $G\alpha_{gust}$-positive cells (57 ± 4%, n = 4) were co-labelled with UEA-1 in the mouse small intestine and these possessed a prominent glycocalyx, distinguishing them from neighbouring epithelial cells (Figure 3.6.14). These $G\alpha_{gust}$– UEA-1 cells were also a mutually exclusive population to those co-labelled for $G\alpha_{gust}$ and either 5-HT or GLP-1 in the mid-jejunum. In the ileum, it was rare to encounter $G\alpha_{gust}$-positive cells that did not possess this prominent glycocalyx labelling, although Figure 3.6.14L depicts a rare exception. In contrast, adjacent epithelial cells that did not possess a glycocalyx did not shown binding of UEA-1.

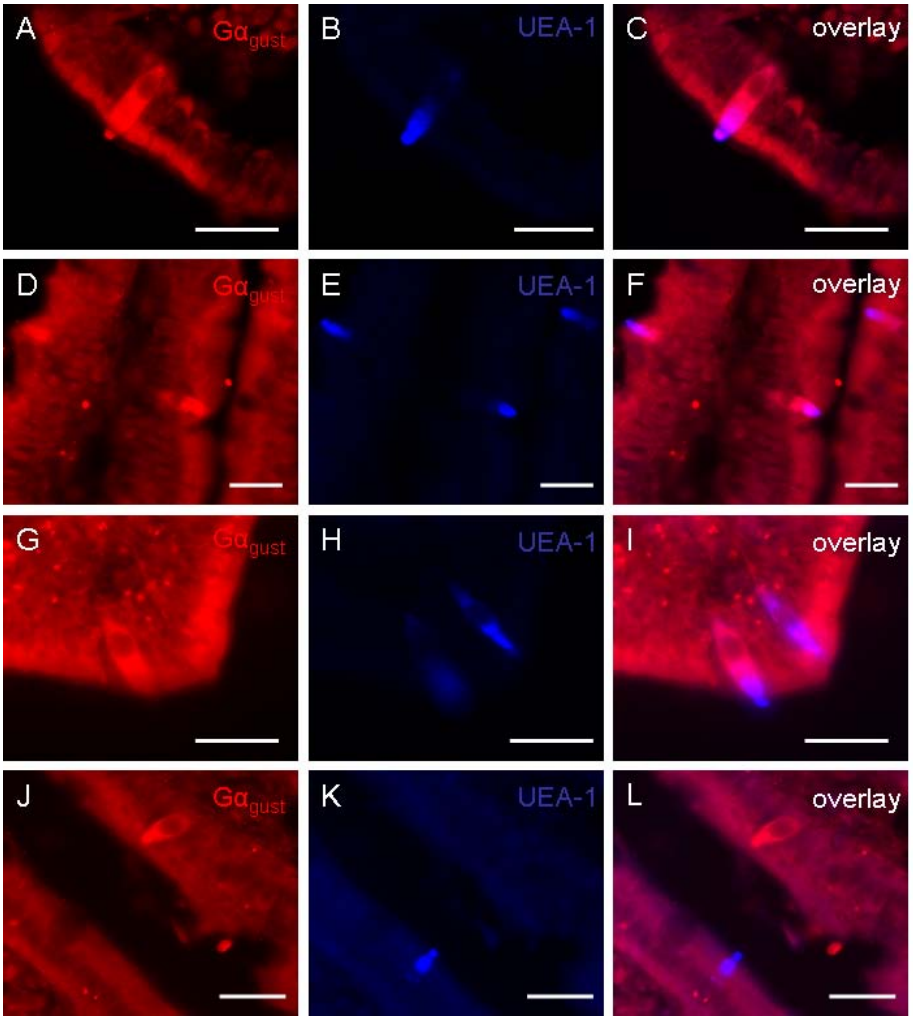

Figure 3.6.14 G**α**$_{gust}$ and lectin Ulex europeaus agglutinin 1 (UEA-1) colabel in mouse epithelial cells. The majority of Gα_{gust} immunopositive cells (57 ± 4%, n =4) throughout the mouse small intestine did not colabel with GLP-1 or 5-HT but bound the lectin UEA-1. UEA-1 label (blue fluorescence, B and E) was strongly concentrated at the apical tip of Gα_{gust}-positive cells (red fluorescence, A and D) and absent from surrounding epithelial cells. Composite images, C and F, confirm UEA-1 binding at the tip of Gα_{gust}-positive cells. UEA-1 label in the mouse intestine was also evident in epithelial cells which did not express Gα_{gust}, a single label UEA-1 positive cell can be seen near a Gα_{gust}-UEA-1 colabelled cell (I). Only a small number of examples of Gα_{gust}-positive cells in the distal small intestine were observed that did not display obvious UEA-1 binding at the apex (L). Scale bars = 50μm.

5-HT, GLP-1 and UEA-1 expression relationships in the small intestine epithelium

Preliminary double-label experiments using 5-HT and GLP-1 primary antibodies on sections of mouse small intestine were performed which demonstrated that GLP-1 and 5-HT labelling was present in mutually exclusive cell populations. In double-label experiments with UEA-1 and either 5-HT or GLP-1, however, UEA-1 binding was detected in rare cells that expressed either 5-HT or GLP-1 (Figure 3.6.15), however no formal quantification of these cell populations was undertaken. Importantly, this co-expression pattern was not detected for epithelial 'taste' cells that expressed $G\alpha_{gust}$-UEA-1 (see below).

$G\alpha_{gust}$ is expressed in different epithelial cell populations in the jejunum

Epithelial cells that co-expressed $G\alpha_{gust}$-5-HT or $G\alpha_{gust}$-GLP-1 displayed a distinct morphology to single-labelled $G\alpha_{gust}$ cells in the mid-jejunum that did not co-express 5-HT or GLP-1 (Figure 3.6.16). Double-labelled $G\alpha_{gust}$ cells were predominantly spindle-shaped with narrowing at the apex towards a thin tip. The immunolabelling pattern for $G\alpha_{gust}$ in these cells commonly showed as punctate label throughout the cytoplasm. In contrast, $G\alpha_{gust}$ cells immunonegative for 5-HT or GLP-1 were predominantly columnar in shape, showed a broader apex and frequently labelled at the apical tip which extended beyond the brush border membrane. $G\alpha_{gust}$ immunolabelling in these cells was strong and homogenous throughout the cytoplasm.

As described above, UEA-1 did co-label with 5-HT or GLP-1 in a small subset of epithelial cells, however in triple-label experiments ($G\alpha_{gust}$ + UEA-1 + 5-HT or GLP-1) no triple labelled cells were ever seen (Figure 3.6.17). As a consequence cells co-labelled with UEA-1-5HT or UEA-1-GLP-1 never expressed $G\alpha_{gust}$. This indicated that there were two distinct phenotypes of $G\alpha_{gust}$-positive cells in the mouse mid-jejunum, one that

expresses enteroendocrine markers (5-HT or GLP-1) but are UEA-1 negative, and another which labels with UEA-1 but does not co-express enteroendocrine cell markers.

Mid jejunal cell counts, expressed as a percentage of total $G\alpha_{gust}$-positive cells, are represented graphically in Figure 3.6.18a and illustrate the proportions of $G\alpha_{gust}$-positive cell phenotypes in this region. $G\alpha_{gust}$-positive cells counts as a percentage of the phenotype markers used (5-HT, GLP-1 and UEA-1) are shown in Figure 3.6.87b. Although the majority of $G\alpha_{gust}$ positive cells are also positive for UEA-1, $G\alpha_{gust}$ expressing cells represent only 17 ± 2% of total UEA-1 cell numbers, indicating these cells are only a small proportion of the total UEA-1 epithelial cell population. On the other hand, $G\alpha_{gust}$ colabelled cells when viewed as a percentage of 5-HT (24 $\pm$ 2%) or GLP-1 (8 $\pm$ 2%) reflected slightly smaller although similar proportions as when expressed as a percentage of the $G\alpha_{gust}$ cell population (Figure 3.6.18b). This indicates that the $G\alpha_{gust}$ expressing enteroendocrine cell populations represent only a subset of the total number of $G\alpha_{gust}$, 5-HT or GLP-1-expressing cells.

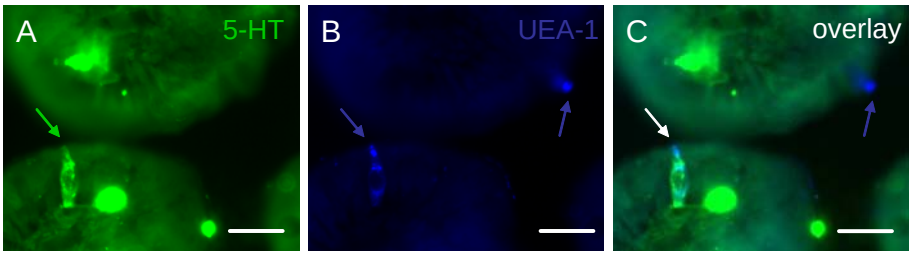

Figure 3.6.15 Lectin Ulex europeaus agglutinin 1 (UEA-1) binding in a subset of enterochromaffin cells in the mouse small intestine.
A proportion of enteroendocrine cells identified by 5-HT in the mouse epithelium displayed UEA-1 binding. A 5-HT immunopositive cell (green arrow, A) contains UEA-1 label (blue arrow, B). Lectin label in the apical region of a 5-HT immunonegative cell (blue arrow, C) can be seen in the same section.
Scale bars = 50μm.

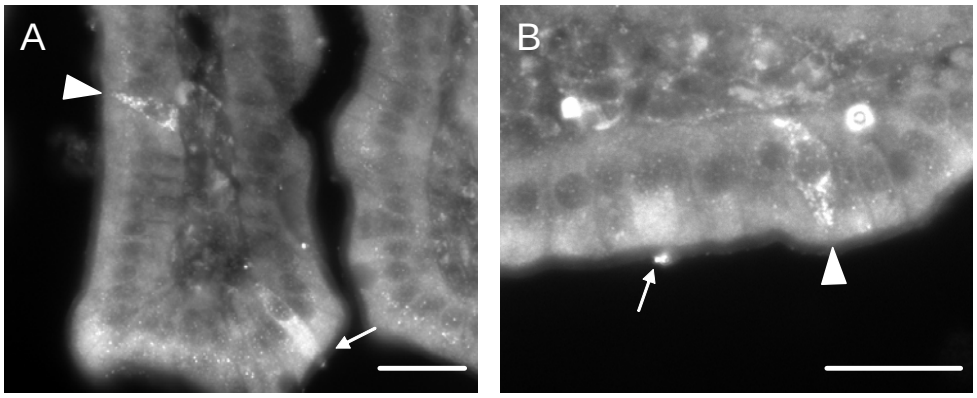

Figure 3.6.16 Typical morphology of different Gα_{gust}-positive cell phenotypes in the mouse jejunum. In the mouse jejunum Gα_{gust}-positive cells appear to belong to two distinct populations, those that express enteroendocrine cell markers 5-HT or GLP-1 and those that bind lectin Ulex europeaus agglutinin 1 (UEA-1). Each Gα_{gust} cell phenotype displayed a distinct morphological appearance. Gα_{gust} cells which co-expressed enteroendocrine cell products (arrowheads) were spindle-shaped with the apical region narrowing towards a thin tip. The immunolabelling pattern for Gα_{gust} in these cells often appeared as punctate label throughout the cytoplasm. Gα_{gust} cells immunonegative for 5-HT or GLP-1 but which bound UEA-1 (arrows), were more columnar in shape, showing a much broader apex and often displayed a strongly immunoreactive apical tip (arrow, B) which extended beyond the brush border membrane. Immunolabelling in this second phenotype was strong and appeared homogenous throughout the cytoplasm. Scale bars = 50μm.

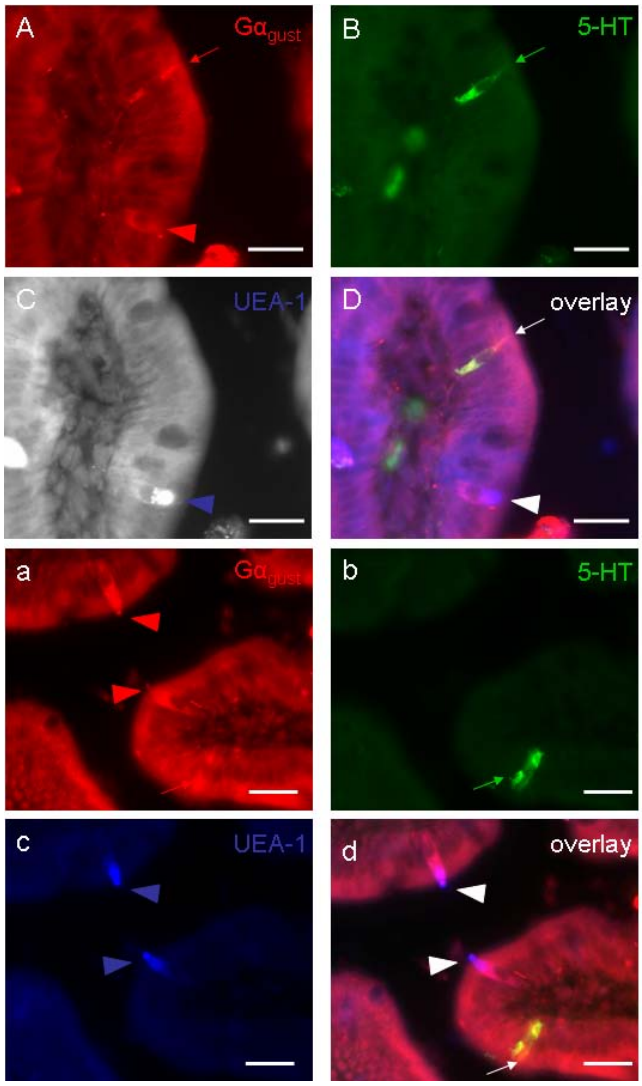

Figure 3.6.17 G**α**$_{gust}$ is expressed in different epithelial cell populations in the jejunum.
Triple label assays for Gα_{gust}, UEA-1 and 5-HT or GLP-1 suggest there are two distinct phenotypes of Gα_{gust} expressing cells in the mouse jejunum. The majority of Gα_{gust}-immunopositive cells throughout the mouse small intestine did not colabel with GLP-1 or 5-HT but bound lectin UEA-1 (blue fluorescence, arrowheads, D and d). A minority of Gα_{gust}-immunopositive cells colabelled with 5-HT (green fluorescence, arrows). Although subsets of 5-HT and GLP-1 immunoreactive cells bind UEA-1 (not shown) cells triple labelled for all three markers were not found, indicating Gα_{gust} is expressed in two distinct populations of epithelial cell in the jejunum. Scale bars = 50μm.

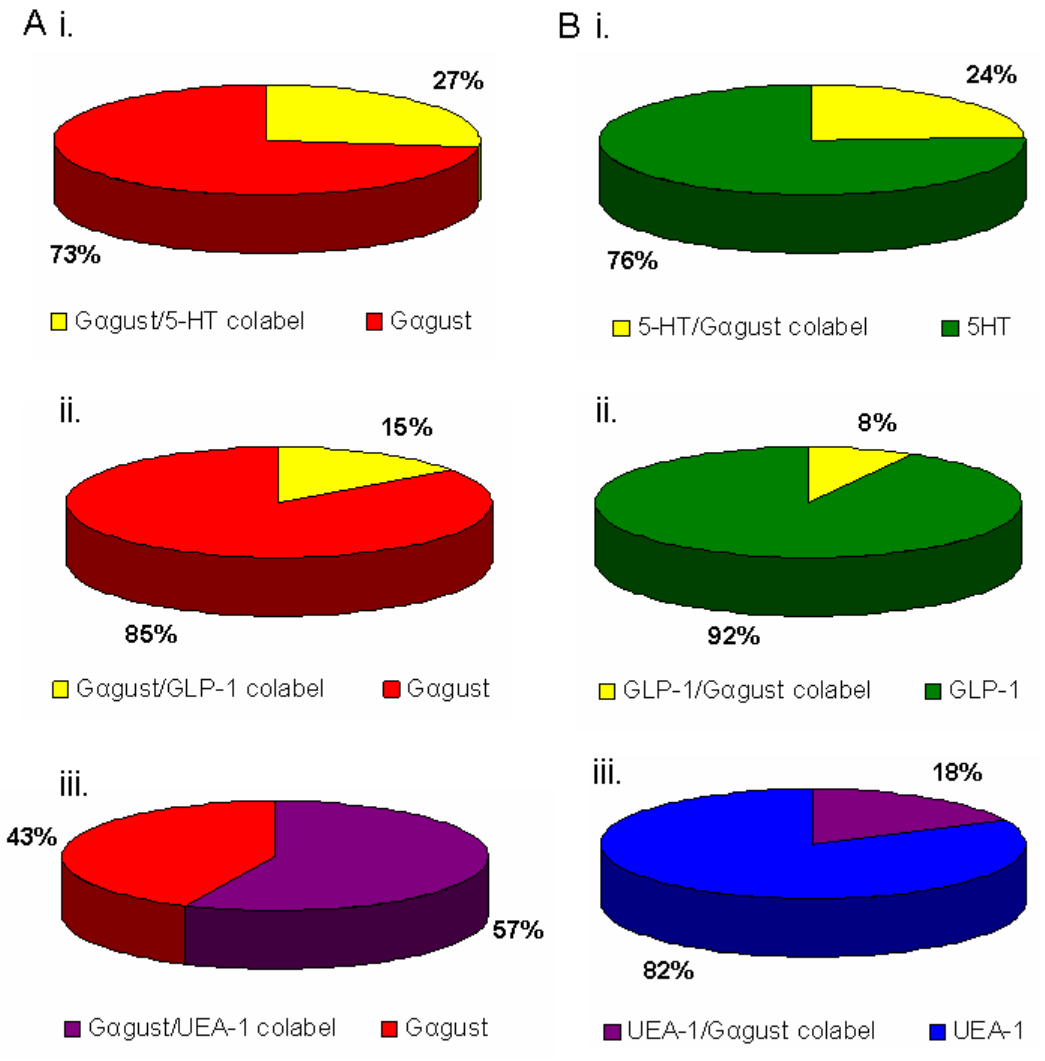

Figure 3.6.18 Gα_{gust}-positive cell populations in the mouse jejunum.
A. Counts per section in the mid jejunum for Gα_{gust}-positive cells show the proportion of colocalisation with 5-HT (i), GLP-1 i(i) and UEA-1 (iii) with yellow (5-HT and GLP-1) and purple (UEA-1) colour representing the colabelled cell population. 27 ± 2% of Gα_{gust}-positive cells contained 5-HT, whereas 15 ± 2% contained GLP-1, N = 4. UEA-1 labelled Gα_{gust}-positive cells made up 57 ± 4% of the total number of Gα_{gust}-positive cells in the region, indicating this was by far the major Gα_{gust} cell phenotype in the region. N = 4.
B. Cell counts for 5-HT (i), GLP-1 (ii) or UEA-1 (iii) show the proportion of Gα_{gust} colabelled cells. The 5-HT-Gα_{gust} and GLP-1-Gα_{gust} colabelled portion represent a similar proportion of the total population when expressed with Gα_{gust} cell type as the denominator, N = 2. However as a percentage of the UEA-1 population Gα_{gust} colabelled cells represented only 17 ± 2% of total cell numbers, indicating that Gα_{gust}-UEA-1 colabelled cells, although a majority of the Gα_{gust} population, make up only a small proportion of the total UEA-1 epithelial cell population. N = 2.

nNOS immunoreactivity in the mouse small intestine

Immunolabeling for nNOS was performed in sections of mouse small intestine to assess expression in $G\alpha_{gust}$-positive cells. Using alternate antibodies, intense labelling for nNOS was observed within neural cell bodies and fibres within the submucosal and myenteric plexus of the small intestine, confirming target specificity of the nNOS antibodies (Figure 3.6.19). However, nNOS was not detected in cells of the intestinal epithelium (Figure 3.6.19), indicating that epithelial cells in the mouse small intestine do not express appreciable amounts of nNOS. As $G\alpha_{gust}$ and nNOS primary antibodies were raised in the same species (rabbit) a double label assay by conventional means was not possible. Therefore, to confirm that $G\alpha_{gust}$ and nNOS were not co-expressed in cells of the villous epithelium consecutive thin sections (5 µm) of mouse jejunum were alternately labelled for $G\alpha_{gust}$ or nNOS. In these, $G\alpha_{gust}$-positive cells were clearly evident but immunolabelling for nNOS immunoreactivity was absent from these labelled cells (results not shown).

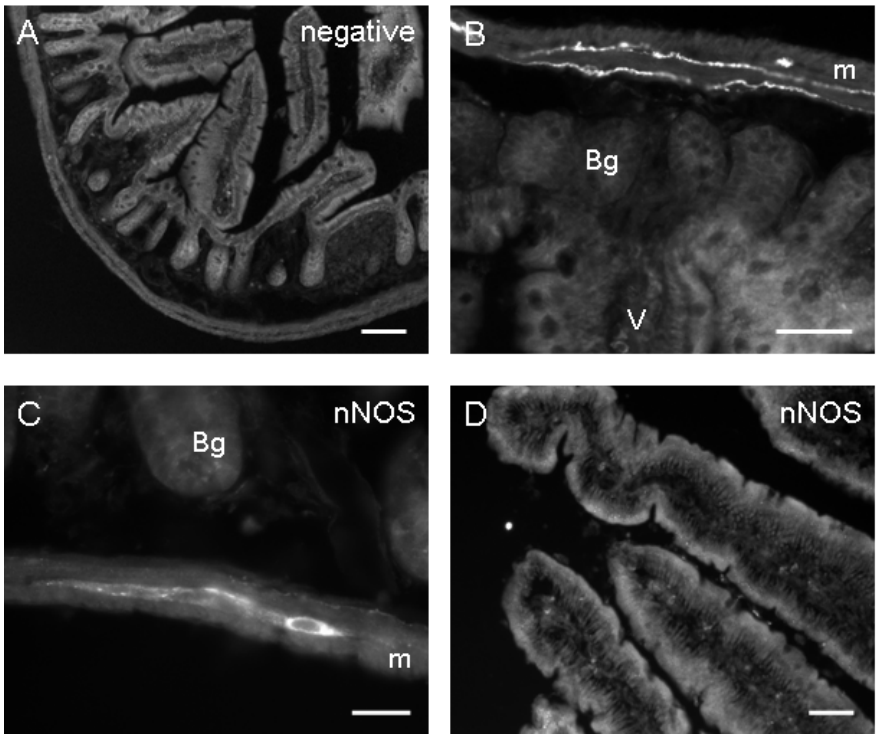

Figure 3.6.19 Neuronal nitric oxide synthase (nNOS) expression in the mouse small intestine. nNOS immunoreactivity could be observed in neuronal cell bodies (C) and fibres (B) in the submucosal and myenteric plexus of the mouse small intestine, which was absent in negative control sections (A). However no immunoreactivity for nNOS was evident in epithelial cells (D), the epithelium appearing identical to negative control sections (A). Scale bars = 50µm (B and C), 100µm (D) and 200µm.

3.7 Discussion

These studies provide the first evidence that the taste specific G-protein $G\alpha_{gust}$ is expressed in distinct epithelial cell populations in the mouse small intestine. These fall into two distinct populations 1) epithelial cells that express enteroendocrine cell markers 5-HT or GLP-1 and 2) those that bind the brush cell marker lectin UEA-1. Because 5-HT and GLP-1 expressing epithelial cells are involved in initiating gastrointestinal reflexes and behavioural responses to luminal nutrients (308, 381) these findings implicate $G\alpha_{gust}$-dependent signalling mechanisms as a potential mediator of intestinal nutrient feedback.

Several characteristics of $G\alpha_{gust}$ immunopositive cells throughout the mouse small intestine were notable. Most prominent was their distribution as singly dispersed cells throughout the epithelium with open access to the lumen. In the majority of $G\alpha_{gust}$ immunopositive cells, particularly the lectin UEA-1 binding-population, an apical tip protruding to the lumen with strong immunoreactivity was obvious, suggesting a specific ability of the these cells to transduce luminal signals. $G\alpha_{gust}$ immunopositive cells were most commonly located in the upper regions of the crypt-villus axis near the villus tip. As luminal contents only have 'efficient' contact with the upper two-thirds to half of the average villus (359) this preferential localisation is significant. These anatomical features combined with the expression of the sensory transduction molecule, $G\alpha_{gust}$, make these cells attractive candidates as one type of primary chemosensory cells for the detection and transduction of luminal nutrient signals.

Although $G\alpha_{gust}$ immunoreactive cells were present throughout the intestinal tract (including the colon) the mid jejunum contained the highest proportion of these cells. This finding is in agreement with previous $G\alpha_{gust}$ expression reported in the small intestine of mice using Western blot, showing highest protein levels in the jejunum (81). $G\alpha_{gust}$ immunoreactive cells were less frequent in the duodenum but were present at

moderate levels in the distal small intestine. Peak expression of chemosensory cells in the mid region of the small intestine may reflect the importance of this length of intestine in exposure in nutrient-evoked reflexes.

Functional experiments to limit nutrient exposure to particular regions of small intestine have been undertaken in a canine model using fistulas inserted at various points in the small intestine (188). This approach has allowed an assessment of the effects of glucose exposure to specific intestinal regions to be tested on reflex slowing of gastric emptying. Exposure of glucose up to the mid point of the small intestine resulted in maximum inhibition of gastric emptying which was dependent on the length of intestine exposed. However regardless of whether glucose was continuously exposed to the entire proximal small intestine or diverted straight to the jejunum, exposure of glucose to this mid jejunal region was important for maximal reflex slowing of gastric emptying. Conversely nutrient exposure to only the initial segment of the duodenum did not stimulate this reflex (53, 188). The importance of the jejunum in initiating nutrient-induced reflexes has also been observed in humans (218). Gastric emptying was faster when diverted away from the region of jejunum beyond the ligament of Treitz whereas infusion of carbohydrate beyond this region resulted in a greater delay in gastric emptying.

Why reflex slowing of gastric emptying due to intestinal glucose requires exposure of the jejunum may be explained by the relative number of chemosensory elements in each intestinal region. $G\alpha_{gust}$-expressing cells, identified in this study displayed a regional specificity that predicted the length dependence of the effects of glucose exposure on gastric motility. Molecular studies outlined in Chapter Two also suggested that the jejunum was a preferential site for sweet taste signalling, based on expression levels of the sweet taste receptor T1R2. $G\alpha_{gust}$-immunoreactive cells have recently also been identified in the epithelium of the entire human gastrointestinal tract (294), with most prominent expression apparent in the colonic mucosa. Regional expression of $G\alpha_{gust}$-positive cells in humans may prove be similar to that in mouse, however

whether fewer cells are present in proximal compared to mid-distal small intestine will be difficult to answer due to accessibility of tissue.

Enteroendocrine cells represent less than 1% of the total number of intestinal epithelial cells but collectively form the largest endocrine organ of the body, releasing more than 20 known hormones (282) that have key gastrointestinal and systemic roles. The 5-HT-secreting enterochromaffin cells make up the largest enteroendocrine cell subtype and 5-HT is an important paracrine signalling molecule to both intrinsic and extrinsic neurons in the gut (105). 5-HT is implicated in gastrointestinal reflex responses to nutrient and is released from enteroendocrine cells in response to carbohydrate, and can activate vagal afferent endings in the rat intestine (381). Intestinal vagal afferents also express 5-HT_3 receptors and a 5-HT_3 receptor antagonist can abolish the inhibition of gastric emptying induced by small intestinal glucose in rats (269).

The incretin hormone GLP-1 also modulates intestinal nutrient-evoked reflexes; it is expressed in L-cells predominantly located in the ileum and colon but also those present in the proximal intestine (345). The prevailing postprandial action of released GLP-1 on gastrointestinal function is to delay gastric emptying (235). The peripheral actions of GLP-1 on gastric motility are abolished by vagal afferent denervation (155) and GLP-1 receptors have been identified in the rat nodose ganglion (234), indicating that vagal afferent terminals in the periphery receive chemosensory information via peripheral GLP-1 receptors.

This evidence outlines roles for 5-HT and GLP-1 in nutrient-evoked gastrointestinal reflexes but the exact identity of transduction molecules linking epithelial detection of luminal carbohydrates to transmitter release have not been elucidated. The taste transduction pathway/s which subserve this function on the tongue is one potential mechanism, and may provide a precedent for nutrient-induced cellular depolarisation and signalling in chemosensory cells further along the alimentary tract. However the data obtained in this study suggest that 5-HT and GLP-1 may be released via both $G\alpha_{gust}$-dependent and –independent pathways.

Only a minority of each of these identified cell types co-express $G\alpha_{gust}$, indicating that a taste-like transduction pathway could operate in only a subset of enterochromaffin and L-cells. Enterochromaffin cells and other enteroendocrine cell subtypes in the intestinal epithelium do not form direct synapses with nerve fibres (18, 355). The rapid turnover of the intestinal epithelium means that permanent synapses of vagal afferents with maturing enteroendocrine cells are unlikely. 5-HT and other endocrine mediators secreted from the epithelium must therefore use paracrine signalling to activate adjacent or distant nerve fibres (18, 355). This anatomical relationship may compensate for the lack of direct input to target cells by hypersecretion of 5-HT from enterochromaffin cells in response to stimuli (105). In fact, local concentrations of mucosal 5-HT appear very high (19) and it is conceivable that 5-HT, GLP-1 or other mediators secreted from only a subset or portion of specific cells may be able to activate neural reflexes. Accordingly, it can be speculated that $G\alpha_{gust}$-5-HT and $G\alpha_{gust}$-GLP-1 cell populations subserve specific nutrient-evoked gastrointestinal reflexes. The notion that enteroendocrine cells may possess diverse transduction mechanisms for nutrient detection and signalling has precedent, as it has been shown that different inositol trisphosphate receptor types are expressed by subgroups of cells within different enteroendocrine subtypes (357). The identity of distinct populations of $G\alpha_{gust}$ taste cells equipped with 5-HT and GLP-1 in the proximal small intestine indicates that at least two different mechanisms are likely to be involved in the triggering of transmitter release from enterochromaffin and L-cells. But the release of 5-HT and GLP-1 by taste transduction mechanisms is probably confined to the mid jejunum in mice.

A key finding in this study was that the overwhelming majority of $G\alpha_{gust}$ cells along the longitudinal axis of the small intestine bound UEA-1, the L-fucose binding lectin, at the apex or glycocalyx of the cell. UEA-1 binding has been shown to predominantly label brush cells in the mouse epithelium (102, 104). UEA-1 is also reported to label a small subset of enteroendocrine cells containing 5-HT and peptide YY (which is also expressed in L cells) in the ileum and caecum of various species including mice (103) and in the current study binding of UEA-1 was observed in subpopulations of identified enteroendocrine cells. However, in the

context of $G\alpha_{gust}$ signalling, no triple-labelled $G\alpha_{gust}$-UEA-1-5-HT or $G\alpha_{gust}$-UEA-GLP-1 cells were seen whatsoever, indicating that UEA-1-5-HT cells do not signal nutrient via $G\alpha_{gust}$ and supporting a clear division of $G\alpha_{gust}$ cells into UEA-1 binding or enteroendocrine subtypes. In this study UEA-1 bound singly dispersed cells throughout the intestinal epithelium. It has been suggested that brush cells are a relatively rare cell type within the small intestine; for example, electron microscopy studies performed in transverse sections of the mouse small intestine reported only two brush cells identified over twelve villi on the basis of ultrastructural features (104). UEA-1 labelled cells were more common in the current study than this previous report and may reflect labelling of multiple cell types, including those immunopositive for $G\alpha_{gust}$. In the absence of electron microscopy to confirm ultrastructural features, however, it can be speculated that the subset of UEA-1 cells co-labelled for $G\alpha_{gust}$ here, represent mouse intestinal brush cells. Brush cells in the intestine have been proposed to have chemosensory functions and possess a characteristic glycocalyx, an anatomical feature shared by chemosensory epithelial cells in other sensory organs, including the nasal cavity and tongue (342, 363). In this study a consistent morphological feature of the $G\alpha_{gust}$-UEA-1 cell population was cell shape and the presence of a specialised glycocalyx, in comparison to surrounding enterocytes, supportive of such a role.

Also to be considered is the varying immunolabelling pattern of $G\alpha_{gust}$ within the two cell populations (enteroendocrine and brush) and whether this may relate to potential functions of $G\alpha_{gust}$ within these different cell types. It is possible that the more punctate appearance of labelling in the enteroendocrine cell groups reflects the intracellular storage of the protein in a non-functioning form. This could suggest that activity is depended on the localisation of the $G\alpha_{gust}$ protein and perhaps the taste transduction pathway is not accessible or is functional in the normal state of the enteroendocrine cell. However this explanation for this observed pattern of immunolabelling is only speculation and it may simply reflect the appearance of labelling in differenct cell types.

In the rat stomach and pancreas, brush cells have been shown to express high levels of nNOS by immunolabelling (179) suggesting NO may be used by these cells as a signalling molecule to activate afferent nerves or other intermediary cell types within the epithelium (133). However in the present study nNOS could not be detected within the mouse epithelium. It appears therefore that the NO signalling capability of brush cells may be organ or species dependent, and that other signalling mechanism(s) may be responsible for transmission of chemosensory signals from $G\alpha_{gust}$-UEA-1 cells.

Subsets of different epithelial cell types (enteroendocrine and brush) are equipped to utilize $G\alpha_{gust}$-dependent signalling in the mouse jejunum. Intestinal taste transduction may release 5-HT, GLP-1 from enteroendocrine cells or non-nitrergic mediators from brush cells however it is likely that this nutrient detection system is only one of such that is operating in the gut. The observations that 5-HT and GLP-1 are not coexpressed support existing reports that 5-HT and GLP-1 are distinct cell lineages in mouse intestine (291). However within each of these cell types, it is possible that other mediators may be released via $G\alpha_{gust}$-dependent signalling. Although $G\alpha_{gust}$ cells labelled with 5-HT and GLP-1 were not quantified in the same sections, cell counts in the mid-jejunum indicate that 99% of the total $G\alpha_{gust}$ immunopositive cell population were labeled with either 5-HT, GLP-1 or UEA-1. It is likely that other enteroendocrine mediators may be released by $G\alpha_{gust}$-dependent signalling within the cell populations defined by $G\alpha_{gust}$-5-HT or $G\alpha_{gust}$-GLP-1 labelling. Indeed, dual GLP-1-peptide YY and GLP-1-GIP cell phenotypes have been described in the porcine, rat and human intestine (229, 345). Furthermore, there is potential for co-release of substance P from $G\alpha_{gust}$-5-HT cells in response to intestinal nutrient (291).

It is important to note that $G\alpha_{gust}$ signalling pathways in the gut may subserve detection of other classes of macronutrient besides carbohdrate such as protein (umami taste) and bitter tastants such as drugs, toxins or bitter nutrient (333). Expression of specific sweet taste receptors would need to be investigated to determine the proportion of $G\alpha_{gust}$ cells that are capable of detecting carbohydrates; unfortunately a lack of

quality antibodies for the T1R2 receptor precluded investigations by this method. It is interesting to note, however, that in preliminary double-label assays in jejunal sections using antibodies for other taste molecules with 5-HT a proportion of T1R3 or $G\gamma_{13}$ immunopositive cells co-expressed 5-HT, in accord with $G\alpha_{gust}$ findings.

In humans, respiratory tract brush cells are infrequent compared to those in rodents (279) and a recent report in human small intestine biopsies (228) suggest this may also be the case in the gastrointestinal tract. $G\alpha_{gust}$ expression in humans may therefore be present in different intestinal cell populations. A first report of $G\alpha_{gust}$ expressing cell types in the human gastrointestinal tract recently showed that labelling for $G\alpha_{gust}$ in the colon coincides with labelling for peptide YY and GLP-1 (294) and a more recent study has demonstrated $G\alpha_{gust}$ in human duodenual L cells (159). However other subpopulations and expression patterns in the jejunum, a potentially more relevant site for initiating nutrient-based motility reflexes, have yet to be explored.

In conclusion, this investigation provides the first direct evidence of small intestinal enteroendocrine and brush cell subpopulations expressing $G\alpha_{gust}$, and their potential paracrine neurotransmitters in mice. The identification of these distinct $G\alpha_{gust}$ cell subpopulations has substantial implications for understanding the nature of nutrient sensing in the small intestine.

4. EFFECTS OF GLP-1 ON MOUSE GASTRO-ESOPHAGEAL MECHANOSENSITIVE VAGAL AFFERENTS *IN VITRO*

4.1 Summary

Background: The gut peptide glucagon-like peptide-1 (GLP-1) regulates energy homeostasis through a variety of actions including postprandial insulin secretion, satiation and inhibition of gastric motility. GLP-1 released from intestinal L-cells in response to luminal carbohydrates is likely to induce delayed gastric emptying via activation of vagal afferent pathways, rather than through endocrine action in the central nervous system. However a direct effect of GLP-1 on the activity of gastrointestinal vagal afferents has not been demonstrated. *Aims:* To demonstrate a specific role of GLP-1 in intestinal nutrient signalling in the direct activation of vagal afferents by assessing effects of GLP-1 on duodenal compared to gastroesophageal (control) afferents. *Methods:* The responses of mouse gastroesophageal vagal afferents to application of GLP-1 were assessed in an *in vitro* tissue preparation. The responses of two types of mechanosensitive vagal afferent receptor (mucosal and tension) were tested with graded mechanical stimuli prior to and after exposure to GLP-1. Mechanosensitive duodenal vagal afferents in a rat *in vitro* preparation were also assessed for suitability to investigate direct effects of GLP-1. *Results:* Mouse gastroesophageal vagal afferents did not significantly alter their basal firing rates upon application of GLP-1. GLP-1 exposure did not significantly alter stimulus-response curves of mucosal receptors (n = 6) to mucosal stroking or tension receptors (n = 4) to circular stretch compared to control ($p > 0.05$). In the rat upper gastrointestinal preparation vagal afferent units responding to mechanical stimuli were identified in the duodenum. However rapid degradation of the mucosa in the in vitro organ bath meant identified mucosal receptors were only transient and responses were short-lived therefore there was not enough time to assess responses to GLP-1. *Conclusions:* GLP-1 does not directly activate or alter the mechanical responses of mouse

gastroesophageal vagal afferents. However the vagal afferents investigated in this surrogate preparation may not reflect the specific properties of intestinal mucosal vagal afferents. To directly assess the effects of GLP-1 on vagal afferent discharge from endings in the intestinal mucosa, further refinement of an *in vitro* duodenal mucosa tissue preparation or alternatively an *in vivo* study may be necessary.

4.2 Introduction

Glucagon-like peptide-1 (GLP-1), a product of the proglucagon gene, is synthesised in enteroendocrine L-cells predominantly located in but not restricted to the distal gut (84) and plays varied roles in the regulation of energy homeostasis (78, 211, 306). In addition to a postprandial incretin action (enhancing insulin secretion), GLP-1 regulates nutrient processing by the gastrointestinal tract primarily through slowing of gastric emptying (235) and by promoting satiety and reducing food intake and appetite (94, 305).

The major stimulus for GLP-1 release from the intestine is ingested nutrients, specifically carbohydrates and fats (29). GLP-1 primarily stimulates intestinal nutrient-evoked reflexes which inhibit gastrointestinal motor function and slow gastric emptying (148). Subpopulations of GLP-1- and 5-HT expressing enteroendocrine cells in the jejunum (Chapter Three) co-express the taste cell trimeric G-protein subunit $G\alpha_{gust}$, linking a known chemosensory transduction mechanism with potential for release of these substances by nutrient stimuli. However only a minor portion of L cells express $G\alpha_{gust}$ and therefore the amount of GLP-1 released by direct 'tasting' of the luminal contents may have specific local effects on adjacent intestinal structures, such as mucosal sensory nerves. However, unlike 5-HT which is known to directly activate intestinal vagal affrents (381), direct stimulation of mucosal afferents by GLP-1 has not been demonstrated.

GLP-1 plays a role in central nervous system (CNS) functions and widespread expression of both GLP-1 and its receptor has been reported within diverse regions of the CNS, including the hypothalamus and

dorsal vagal complex (161, 178, 325). Central administration of GLP-1 both slows gastric emptying and reduces food intake (155, 344, 350). Although peripheral GLP-1 has access to the CNS through the blood brain barrier (164, 248), a solely central site of endocrine action of GLP-1 to slow gastric emptying is unlikely due to several lines of evidence. Firstly the bioactive form of GLP-1 (7-36 amide) is rapidly degraded in the circulation having a half-life of 1-2 min (71, 169). This rapid metabolism of bioactive GLP-1 occurs by the proteolytic enzyme dipeptidyl peptidase-4 (DPP-4) (213) which is widely expressed in multiple tissues but significantly, on endothelial cells that line the capillaries within the intestinal mucosa where GLP-1 is secreted (115). At least half the amount of released GLP-1 is in its inactive form before it reaches the portal vein (115) and a further 40% may be degraded in passage through the liver (72) and beyond this in the systemic circulation. DPP-4 is also present as a soluble circulating protein in addition its localisation to the endothelial surface (212). This suggests that the vast majority of intestine-released GLP-1 must be biologically inactive by the time it has opportunity to cross the blood-brain barrier into the CNS.

Although GLP-1 can cross the blood brain barrier, peripheral administration of an impermeant albumin-linked GLP-1 receptor (GLP-1R) agonist can activate CNS neurons involved in the inhibition of gastric emptying (10). Furthermore dennervation of the vagal trunks using the sensory neurotoxin capsaicin abolishes the peripheral action of GLP-1 on gastric emptying (155). This suggests that ascending vagal neural pathways are important for the effects of peripheral GLP-1 on gastric emptying. This view is supported by reports that GLP-1R (the only known GLP-1 receptor) is expressed in the rat nodose ganglion (234) and therefore the GLP-1 receptor may be expressed on vagal afferent terminals that innervate the intestine. Furthermore hepatic vagal afferents appear to be receptive to the appearance of GLP-1 in the portal vein (231), dose-dependently increasing their firing rate in response to GLP-1 perfusion. Therefore it appears likely that vagal afferents can signal the presence of GLP-1 via an increase in afferent discharge at least in the portal vein. However as more than half of bioactive GLP-1 is degraded in the mucosal capillaries before it reaches the portal vein, it is likely that GLP-1 is directly detected by vagal afferents in the mucosa

adjacent to its intestinal release site. However a direct action of GLP-1 on gastrointestinal vagal afferents has not been demonstrated.

Electrophysiological multi-fibre recording techniques allow vagal afferent discharge to be assessed in response to mechanical and chemical stimuli. Originally refined in whole animal *in vivo* preparations (24, 59, 69) recent development of *in vitro* tissue preparations (28, 200, 251, 358) offer several advantages when assessing chemosensitive properties of vagal afferents. Investigations in an *in vitro* preparation can be more highly controlled and replicable, there are no confounding effects of anaesthesia, receptive fields are more easily accessible and applied chemical agents can be precisely controlled in terms of concentration and direct site of application to the receptive field. Additionally observed responses are less likely to occur secondarily to motility responses or release of other endogenous mediators. In our laboratory an *in vitro* preparation for recording from vagal afferents innervating the gastroesophageal region is well established in the mouse and was used to investigate properties of gastroesophageal afferents (252, 254, 255, 326). A specific role for GLP-1 in intestinal nutrient signalling could be demonstrated by showing direct activation of intestinal vagal afferents by application of GLP-1 while showing negligible effects on vagal afferents innervating other regions of the gastrointestinal tract (such as the gastroesophageal junction) that do not contain native L cells. The feasibility of investigating the effects of GLP-1 on vagal afferents in the small intestine *in vitro* was assessed for comparison to results from a control gastroesophageal preparation.

4.3 Aim

To assess whether GLP-1 directly activates vagal afferents to further understand its role in intestinal nutrient signalling.

4.4 Specific hypotheses

1. GLP-1 will not alter afferent discharge or potentiate the mechanosensitive responses of mouse gastroesophageal vagal afferents *in vitro*.

2. An in vitro gastrointestinal preparation allowing vagal afferent recordings from the duodenum in rats can be developed to demonstrate specific effects of GLP-1 on duodenal vagal afferents.

4.5 Materials and methods

Experiments were performed using adult male C57BL/6 mice aged 7-10 weeks or Sprague-Dawley rats weighing approximately 200g, housed conventionally with free access to water and a standard laboratory rodent diet. All studies were performed in accordance with the Australian code of practice for the care and use of animals for scientific purposes and with the approval of the Animal Ethics Committees of the Institute of Medical & Veterinary Science (Adelaide, Australia) and the University of Adelaide or Flinders Medical Centre and Flinders University (Adelaide, Australia).

4.5.1 *In vitro* mouse gastroesophageal vagal afferent preparation

Female C56/BL6 mice aged 7-10 weeks (n = 10) were killed by CO_2 inhalation. A midline incision was performed and the stomach, esophagus with attached vagal nerves, heart and lungs were removed and placed in ice-cold modified Krebs solution bubbled with carbogen (95% O_2/5% CO_2). During the dissection, temperature of the Krebs solution was maintained at <4ºC to prevent metabolic degradation of tissues. The heart and lungs were removed under a dissecting microscope avoiding the vagal nerve trunks. Both vagal

nerves were then dissected free from connective tissue holding them to the upper esophagus and the preparation was opened longitudinally along the esophagus and the greater curvature of the stomach, keeping both nerves intact. The dorsal half of the stomach was removed and the preparation pinned out flat mucosa side up along the straight edge of a Perspex organ bath (dimensions 6 cm x 2.5 cm x 1.2 cm) lined with Sylgard (Dow Corning Corp., Midland, MI). This chamber was superfused via a peristaltic pump with oxygenated Krebs solution warmed to 34ºC. The vagal nerves were extended from the organ bath into an adjacent recording chamber (dimensions: 3.7 cm diameter, 1.2 cm deep) through a small hole in the removable sliding 'gate' separating the two compartments. The nerve trunks were laid on a small glass plate and the recording chamber was filled with paraffin oil (Figure 4.5.1). With the aid of a dissecting microscope the vagal nerves were desheathed and fine forceps were used to tease apart the nerve trunk into 8-16 finer bundles. The nerve bundles were placed one at a time onto a platinum recording electrode. A platinum reference electrode was rested on the glass surface in a small pool of Krebs solution adjacent to the recording electrode.

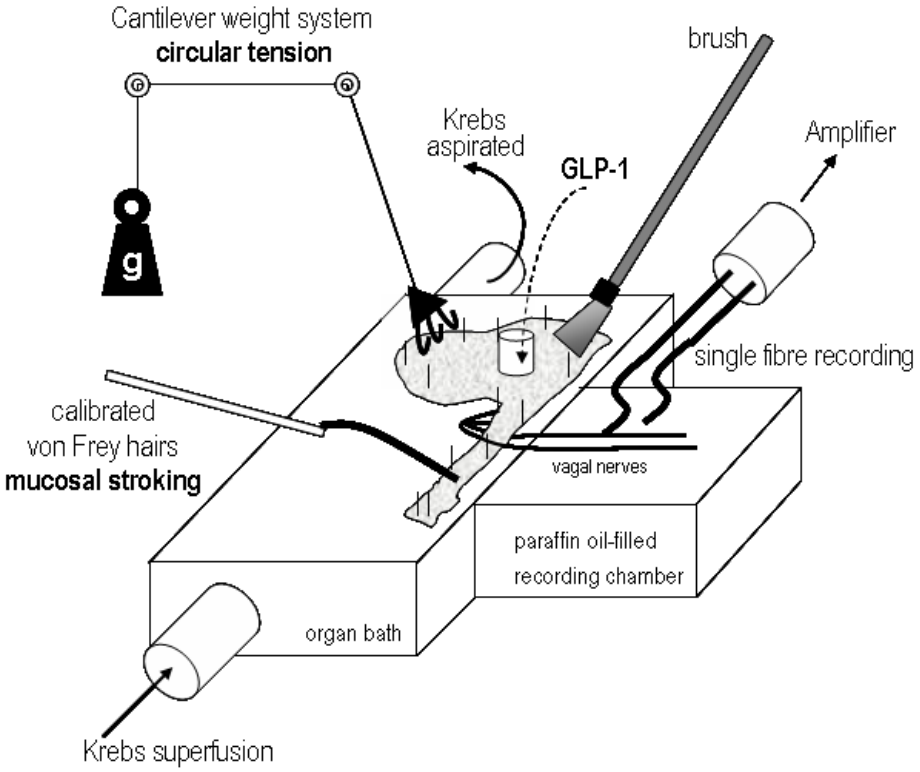

Figure 4.5.1 Schematic diagram of the apparatus used to obtain single fibre recordings from mouse gastroesophageal vagal afferents *in vitro*.
The flat tissue preparation consisting of esophagus and ventral stomach was pinned with the mucosa upwards in a Perspex chamber superfused and aspirated with warmed Krebs solution. The vagus nerves were passed under a gate into a second oil-filled chamber where individual teased nerve bundles were placed on a recording electrode. Mechanically sensitive receptive fields were identified by passing a brush over the tissue surface. The mechanosensitivity of individual units was further assessed using calibrated von Frey hairs. Circular tension was applied via a cantilever weight system via a hook in the tissue adjacent to the receptive field. GLP-1 was applied to a metal ring placed and sealed over the receptive field.

Characterisation of gastroesophageal vagal afferent properties

Mechanically sensitive receptive fields were located by systematically stroking the mucosal surface of the preparation with a fine brush. To classify the identified receptive field two distinct forms of mechanical stimuli were applied: 1) mucosal stroking using fine calibrated von Frey hairs and 2) circular tension applied through weights on a cantilever and claw system attached to the tissue adjacent to the receptive field. Mechanical responses of vagal afferents in this preparation have previously been characterised into two distinct fibre types (252, 254, 255, 326). These are 1) mucosal receptors and 2) tension receptors. Mucosal receptors respond to mucosal stroking but not circular tension whereas tension receptors respond to both mucosal stroking and circular tension.

The stimulus-response function of each afferent unit was characterised according to the following protocols. Mucosal stroking was performed with calibrated von Frey hairs of 10, 50, 200 and 1000 mg force. The bent tip of the von Frey hair was moved over the receptive field to obtain a response. The number of action potentials elicited per stroke of the calibrated force was recorded but to minimise error due to the small size of the receptive field responses to the middle 8 of 10 standard strokes given at 1 s intervals were averaged for analysis. Tension-response curves were obtained for those units that responded to circular stretch. Tension was applied through a claw made from bent dissection pins attached via thread to a pulley and cantilever system. The claw was hooked into an unpinned portion of tissue adjacent to the receptive field and to balance the opposite end of the cantilever calibrated weights of 1, 3 and 5 g were applied in randomised order for 1 minute periods with a 1 minute rest between application of weights.

Application GLP-1 and assessment of effects on gastroesophageal vagal afferents

After the mechanical properties of individual vagal afferent units was established the effects of GLP-1 on spontaneous firing and mechanical sensitivity were determined. GLP-1 was assessed at a range of concentrations from 10^{-8} to 10^{-5}M based on potencies previously published (231, 232). A metal ring with edges sealed with silicon grease was placed on the preparation over the receptive field. Krebs solution inside the ring was aspirated out and ~100µL of GLP-1 (10^{-8}M) was added to the ring and allowed to equilibrate for 10 minutes to allow thorough penetration into all layers of tissue. Spontaneous activity was recorded before and during the GLP-1 incubation. Immediately after the removal of the ring the stroke-response and tension-response curves were re-determined. This protocol was repeated for GLP-1 at increasingly higher doses (10^{-7} – 10^{-5}M). In 3 separate experiments a positive control condition was performed to confirm the integrity of the preparation. After the completion of the GLP-1 protocol on a mucosal afferent, NMDA was applied for 10 minuntes to the receptive field, at a concentration previously demonstrated to potentiate the response of mucosal afferents, and mechanosensitivity reassesssed.

Data recording and analysis

Afferent impulses generated in nerve fibres placed on the platinum recording electrode were amplified (DAM 50; World Precision Instruments, Sarasota, FL, USA), filtered (Band pass filter-932; CWE Inc., Ardmore, PA, USA) and sampled using a 1401 interface (Cambridge Electronic Design, Cambridge, United Kingdom). The amplified signal was visually monitored and recorded on using Spike 2 software (Cambridge Electronic Design, Cambridge, UK) on a PC with on-line audio monitoring through an audio mixer (Stereo Sound Mixer CE, Jaycar Pty Ltd, Adelaide SA). Off-line analysis was performed using the Spike 2 software with single units discriminated on the basis of action potential shape, duration and amplitude.

Responses to stroking were calculated as the mean number of action potentials generated during the each stimulus. Response profiles to stretch were calculated as the mean number of spikes per 5-second bin over the 60 seconds of applied tension. Spontaneous nerve activity was calculated as the mean number of spikes per 5-second bin over the periods between and during GLP-1 incubations. Data are expressed as mean ± SEM of responses of individual afferents. Data was analysed using Prism 4 software (GraphPad Software, San Diego, CA). Statistical analysis to assess differences between stimulus-response curves was performed by two-way analysis of variance (ANOVA). Analysis of spontaneous nerve activity before and during GLP-1 application was tested by one-way ANOVA. $P < 0.05$ was considered significant.

Drugs and solutions

The composition of the modified Krebs solution used was as follows (mM): 118.1 NaCl, 4.7 KCl, 25.1 $NaHCO_3$, 1.3 NaH_2P0_4, 1.2 $MgS0_4.7H_20$, 1.5 $CaCl_2$, 1.0 citric acid and 11.1 glucose. Nifedipine (10^{-6}M) was added to the Krebs superfusate solution to prevent smooth muscle contraction and to eliminate effects secondary to smooth muscle responses. Previous studies have shown that nifedipine has no effect on the mechanical sensitivity of gastroesophageal vagal afferents in this preparation (326).

Glucagon-like peptide 1 (7-36) amide was obtained from Tocris (catalogue no. 2082, Tocris, Bristol, UK). The GLP-1 peptide was prepared as a stock solution in Krebs solution containing 0.01% bovine serum albumin (BSA) (Sigma, Castle Hill, NSW, Australia). Aliquots of stock solution were kept frozen and diluted to final concentrations in Krebs/BSA solution on the day of the experiment.

NMDA, used as a positive control for potentiation of the mechanical response of mucosal units (326), was obtained from Tocris (Tocris, Bristol, UK). NMDA stock solution was diluted with Krebs to a concentration of 10^{-3}M on the experimental day.

4.5.2 In vitro rat duodenal vagal afferent preparation

Male Sprague-Dawley rats (~200g) were anaesthetised with Nembutal (60 mg/kg, i.p., Rhone Merieux Australia, QLD, Australia). The abdomen and thoracic cavity were opened via mid-line incision and the entire viscera including the heart, lungs, esophagus, stomach, intestine, pancreas and liver were removed and rinsed in ice-cold Krebs solution. The tissue was kept in ice-cold oxygenated Krebs solution for dissection, in identical manner to the mouse gastroesophageal preparation. The duodenum was sectioned caudal to the pancreatic attachments and the distal small bowel removed. The liver was removed under a dissection microscope to confirm that vagal common hepatic branch was intact. The heart and lungs were removed and the vagal nerves identified along the thoracic esophagus and dissected free from the connective tissue to the celiac and hepatic vagal branches. The stomach was opened along the greater curvature, the contents removed and the preparation pinned flat. In some preparations the vagal gastric branches were cut caudal to the celiac and hepatic branches and the esophagus and stomach were removed to isolate afferent signals arising from the duodenum without interference from spontaneously firing gastric afferents. Sectioning of the gastric vagal branches is unlikely to significantly reduce the number of duodenal afferents in the preparation as the majority of vagal innervation of the duodenum travels via the hepatic branch (259).

The tissue was pinned in organ bath similar, though larger (12 cm x 6 cm x 2 cm) than that used for the mouse preparation. As with the mouse preparation the vagus nerves were passed into a paraffin-filled recording chamber and teased bundles of vagal fibres were individually placed on the platinum recording electrode and vagal discharges were recorded and monitored using similar equipment as for the mouse gastroesophageal recordings.

Mechanically sensitive receptive fields on the duodenum were identified by a blunt probe used to produce a gentle focal compression over the duodenal tube. In some preparations the duodenum was opened longitudinally along the anti-mesenteric border and pinned as a flat sheet to allow access to the mucosa of the tissue. A blunt probe or brush was used as a mechanical stimulus to search for receptive fields.

4.6 Results

4.6.1 Effects of GLP-1 on mouse gastroesophageal vagal afferents

Receptive fields of gastroestophageal vagal afferent endings were predominantly located in the distal esophagus or the lower esophageal sphincter (LES), with only one or two receptive fields located below the LES in the stomach tissue (Figure 4.6.1C). Single afferent fibres were classified as either mucosal or tension receptors according to their response to mechanical stimulation. Both mucosal and tension receptors responded to mucosal stroking with von Frey hairs in a graded manner to forces of 10 to 1000 mg (Figure 4.6.1). Tension receptors displayed a graded increase in the number of impulses in response to applied loads of 1, 3 and 5 g (Figure 4.6.1B). Single units were classified as mucosal if they responsed to stroking but did not appear to increase their firing rate in response to applied circumferential tension.

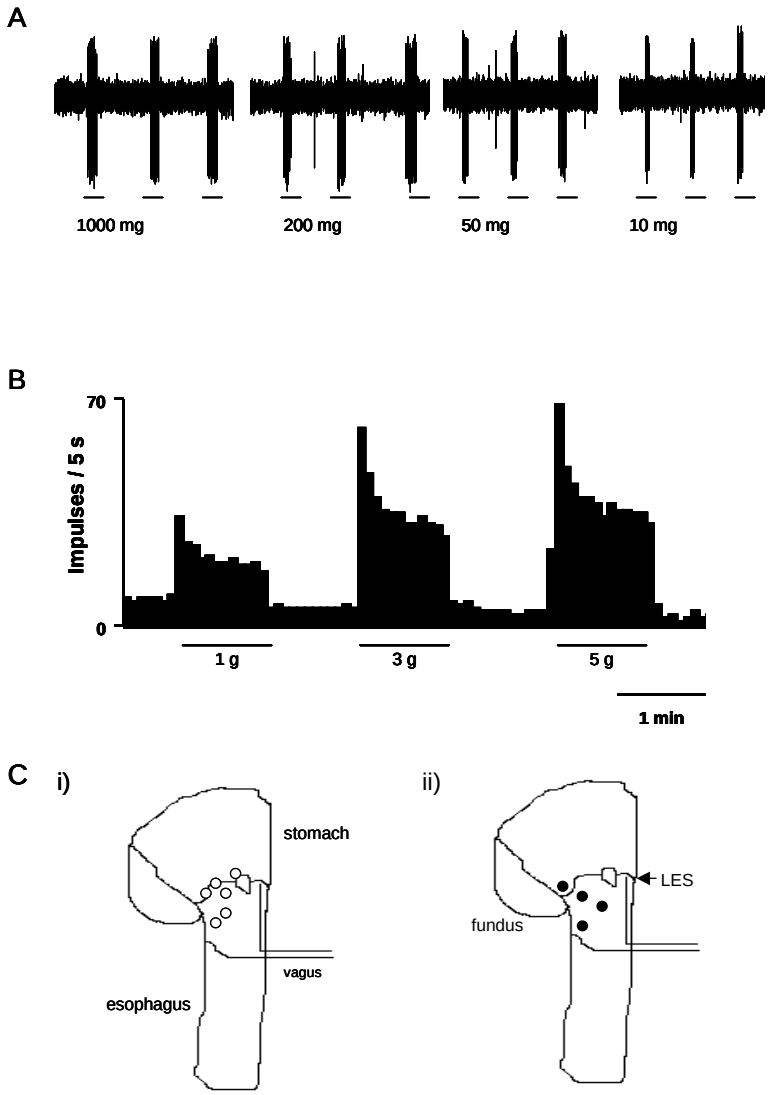

Figure 4.6.1 Responses of mouse gastroesophageal vagal afferents to mechanical stimuli.
Raw trace of the response of a single afferent unit to mucosal stroking with calibrated von Frey hairs (10-1000mg) (A). Discharge rate (impulses per 5 s) of a tension receptor is shown in responses to increasing loads of applied circular tension (B). Mucosal receptors are insensitive to applied tension (not shown) and thus afferents were classified as mucosal receptors if they failed to elicit a response to circumferential tension. Locations of mucosal (i) and tension (ii) receptors assessed in the mouse gastroesophageal preparation (C), each point represencts the location of receptive fields of single afferent fibres in a composite of results from all experiments. Most receptive fields were located in the distal esophagus or on the lower esophageal sphincter (LES).

GLP-1 exposure to either mucosal or tension receptors did not significantly change the spontaneous firing rates of individual units (Figure 4.6.2). Addition of GLP-1 to the ring around the receptive field did not result in an increase in mean rate of impulses generated by individual units over the 10 min time course of incubation at any of the concentrations of GLP-1 used. No significant difference were apparent between firing rates of baseline spontaneous activity and during exposure to any GLP-1 concentration (one-way ANOVA, $p > 0.05$), indicating that GLP-1 does not alter spontaneous firing rate of mouse gastroesophageal mucosal or tension receptors.

The lack of effect of GLP-1 on mucosal and tension receptor responses to mechanical stimulation is illustrated in Figure 4.6.3B. The stimulus response curves to 10 - 1000 mg mucosal stroking were not different in terms of the number of impulses per stroke of mucosal receptors between control conditions and after exposure to any concentration of GLP-1 (10^{-8} – 10^{-5}M) (Figure 4.6.3Bi). This indicates that GLP-1 did not significantly potentiate the mechanical response of mucosal receptors in mouse gastroesophageal tissues. Similar results were obtained for the stimulus response curves of tension receptors to applied loads (Figure 4.6.3Bii). No significant difference in the response to applied loads was found before or after GLP-1 exposure (10^{-8} – 10^{-5}M) indicating that the response of gastroesophageal tension receptors is not altered by GLP-1.

A potentiation of the response of mucosal receptors to mucosal stroking has previously been shown in this preparation following exposure to the NMDA receptor agonist NMDA (326). NMDA was used in several experiments on mucosal receptors after completion of the GLP-1 protocol as a positive control. A significant increase in the number of impulses generated in response to a single mucosal stroke was observed in the presence of NMDA (10^{-3}M) compared to control (two-way ANOVA, $p < 0.05$, Figure 4.6.3A). These positive control results confirm the responsiveness of vagal afferents in the preparation, and that GLP-1 has no significant effect on mouse gastroesophageal vagal afferents.

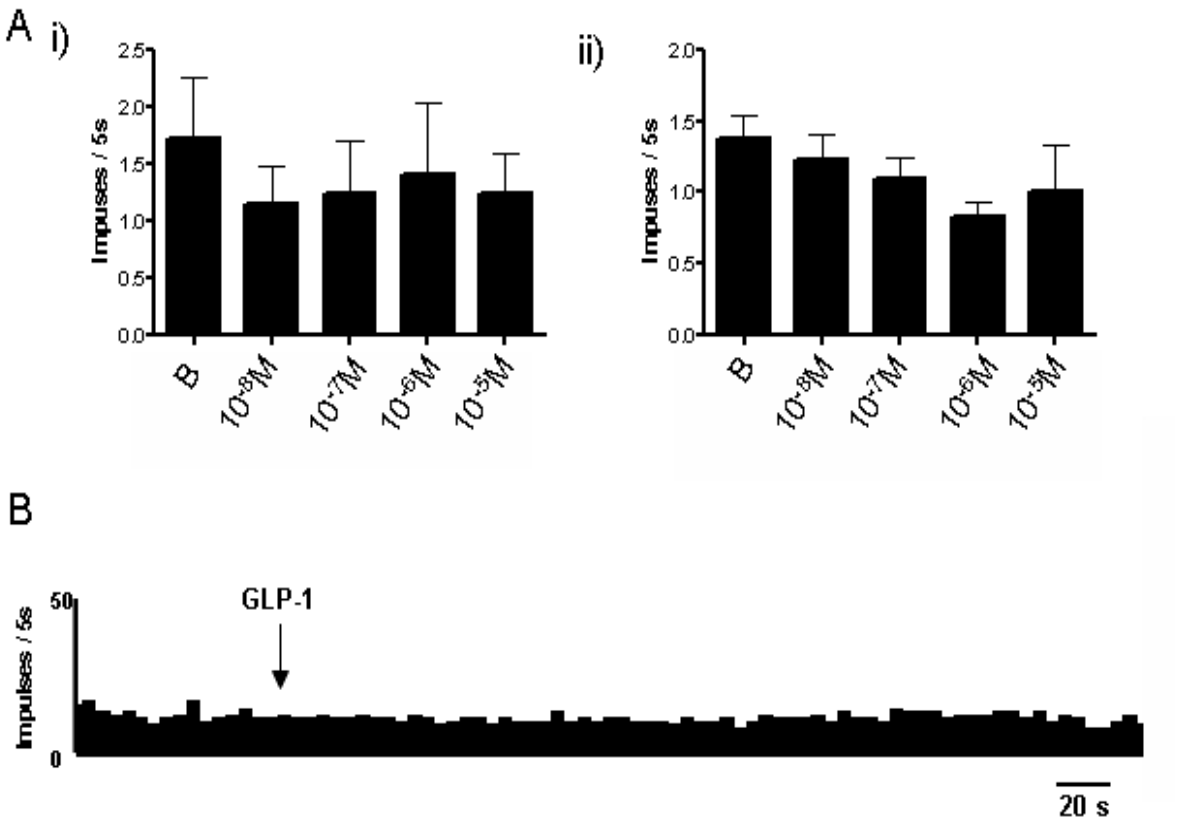

Figure 4.6.2 Response of mouse gastroesophageal vagal afferents to GLP-1.
Mean spontaneous activity (baseline) of mucosal (n = 6) (i) or tension (n = 4) (ii) receptors did not significantly differ during incubation with GLP-1 at any of the concentrations used (A). Representative trace of a mucosal receptor showing spike frequency before and after addition of GLP-1 (10^{-7}M) (B). No change in spontaneous firing rate is seen over the incubation period. B; baseline.

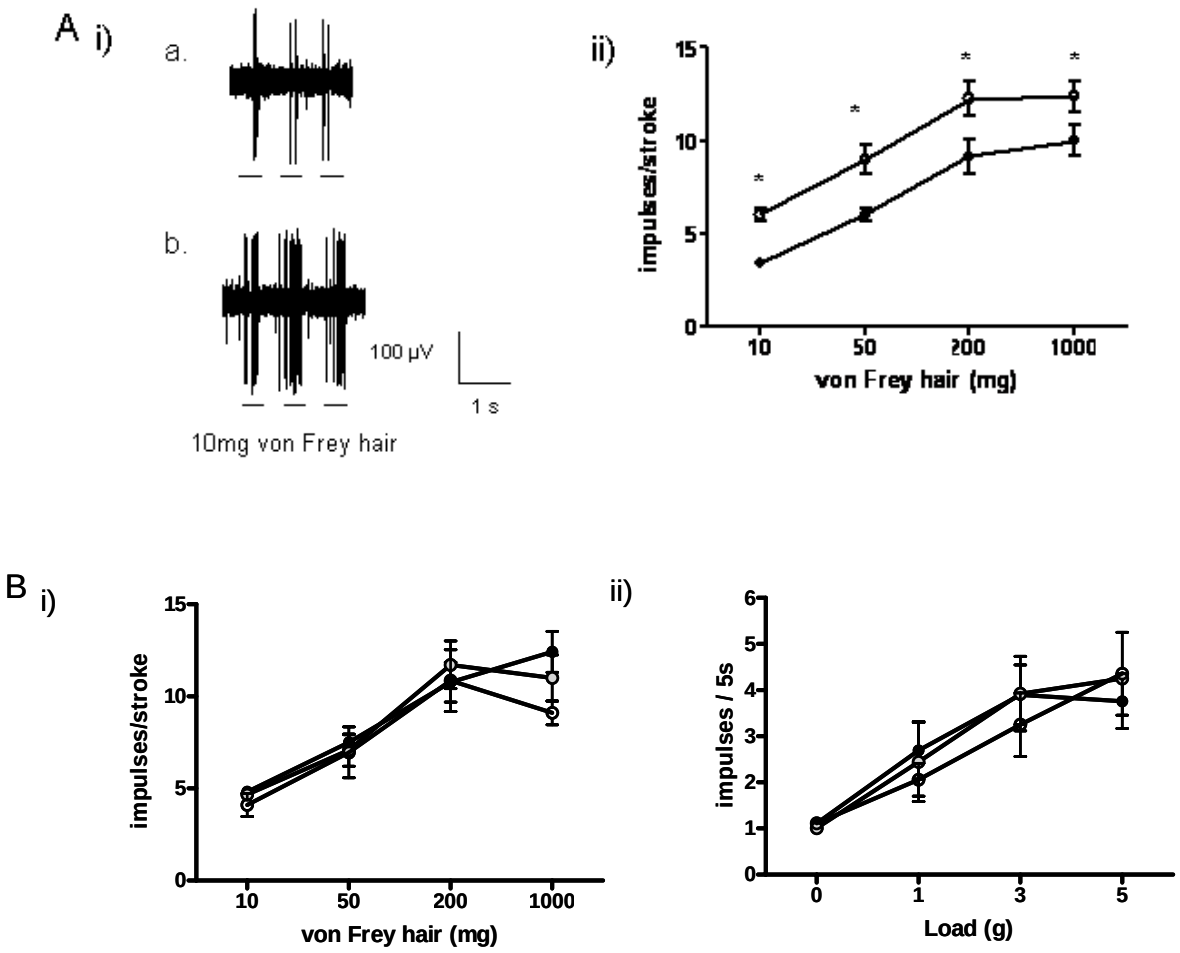

Figure 4.6.3 Effects of GLP-1 on mechanosensitivity of mouse gastroesophageal vagal afferents. In this preparation, NMDA has been shown to potentiate the response of mucosal receptors to stroking and served as a positive control for these studies (A). A raw trace from the original recording (i) shows a mucosal receptor response to mucosal stroking with a 10mg von Frey hair before (a) and after (b) incubation with NMDA (10^{-3}M). The impulses generated in response to stroking with calibrated von Frey hairs of increasing force are significantly greater after NMDA exposure (open circles) than control (closed circles) (* $P < 0.05$) (ii). Exposure to GLP-1 did not alter mechanosensitivity of vagal afferents (B). Both mucosal (n = 6) (i) and tension receptors (n = 4) (ii) did not show any significant difference in response to stroking or circular tension after GLP-1 exposure at any concentration compared to control (closed circles). Only the lowest concentration, 10^{-8}M (grey-filled circles) and highest concentration, 10^{-5}M (open circles) of GLP-1 are shown for clarity.

4.6.2 Assessment of rat duodenal vagal afferents in vitro

In 11 upper gastrointestinal vagal afferent preparations a total of 22 single, mechanically sensitive units were identified in the duodenum by blunt probing. The approximate locations of the receptive fields of these duodenal vagal afferents are represented in Figure 4.6.4. Duodenal units were predominantly found within the first 2 cm of the duodenum beyond the pylorus and in the composite map of experimentally identified units they tended to cluster in this region. The majority of units were identified in recordings from the left (ventral) vagus (producing the common hepatic branch) although a single duodenal unit was identified in the right (dorsal) vagal branch in each of two preparations.

Twelve of the 22 single units showed spontaneous firing, whereas 10 were silent unless mechanically stimulated. Conduction velocities measured in all units were in the range of C fibres ($0.48 \pm 0.09 ms^{-1}$, n = 10).

Two units were found per experiment, on average, with a maximum of 5 identified in one preparation; receptive fields were only identifiable early in the experiment likely due to degradation of duodenal mucosa integrity. While the duodenal mucosa remained macroscopically healthy in cold Krebs solution, it rapidly degraded once the organ bath solution was warmed for nerve recording. With an intact tubular duodenum preparation probing of the serosal surface caused sloughing of the mucosa within the lumen. This detachment of the mucosa continued over the experimental period leaving the duodenal walls thin and clear. When the duodenum was longitudinally opened and pinned flat, any mechanical contact with the mucosa caused large sections of mucosa to detach, leaving only muscle layers. Therefore application of a mechanical stimulus to the mucosa was virtually impossible without destruction of the mucosa itself. On only a few occasions was a mucosal unit able to withstand several light mechanical touches before

responses stopped. In these cases afferent discharge could still be stimulated electrically suggesting that the loss of mechanical response was due to destruction of the afferent ending in the mucosa.

Several strategies were investigated to improve the integrity of the mucosa. Modification of the Krebs solution, including the use of calcium-free (high magnesium) Krebs with and without glucose, the replacement of glucose with L-glutamine (the preferred energy source of enterocytes) and the addition of protease inhibitors to the solution was attempted. Slow perfusion of these Krebs solutions directly into and through the duodenal lumen in addition to the bath solution was also tried. Unfortunately no modification of the Krebs solution or delivery strategy significantly altered the degradation of the mucosa. Even the mechanical force of slow perfusion of Krebs through the lumen detached the duodenal mucosa.

Due to these factors the most successful way to identify mechanically sensitive units was light focal compression of the duodenal serosa with a blunt probe. This action potentially activated mucosal receptors by apposing the mucosal surface, however tension receptors between the muscle layers could similarly be activated by the associated stretching of the duodenal walls. Using this approach, repeat responses (up to 10) to probing could be evoked in a number of single units.

Due to the transient nature of the preparation an investigation of GLP-1 effects on duodenal vagal afferents was not possible. Attempts to test effects of GLP-1 (10^{-9}, 10^{-6}, or 10^{-3}M) by several application methods were tested (n = 6). A ring was placed over the receptive field on the mucosa of the flat duodenum sheet, or GLP-1 was injected into the lumen, with and without restriction of the region containing the receptive field with sutures. No responses to GLP-1 were observed. However these results were not conclusive as the response to probing was lost prior to application of GLP-1 to the ring, suggesting damage to afferent endings. Negative findings with delivery of GLP-1 into the duodenal lumen also could not rule out the

possibility that the receptive field was not exposed, or whether exposure was long enough. It was not possible to apply GLP-1 to the bath directly to assess for any effects without the need for mechanical stimulation due to the GLP-1 being supplied in only small quantities.

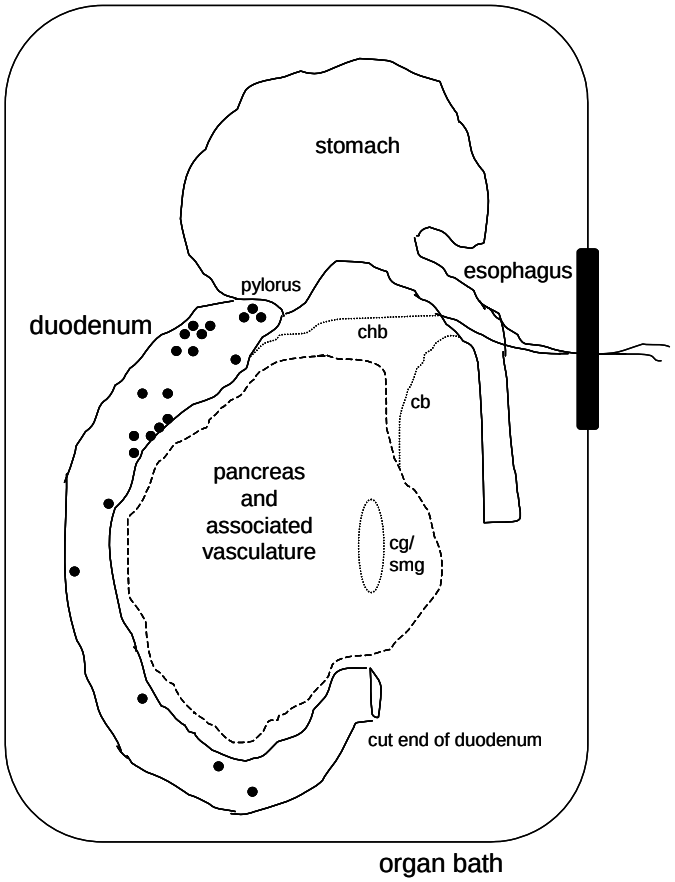

Figure 4.6.4 Schematic distribution of single mechanosensitive receptive fields on the duodenum of the rat.

A typical layout of the rat upper gastrointestinal tissue preparation in the organ bath is shown. The majority of recordings were obtained from fibres in the left cervical vagus which projects through the common hepatic branch (chb) to the duodenum. In some preparations the stomach and esophagus were removed, leaving the isolated duodenum and adjoining hepatic vagal branch intact. Mechanically sensitive receptive fields were identified by blunt probing of the exposed serosal surface of the duodenum. In 11 preparations, 22 duodenal afferent units with distinct receptive fields were identified. Each point (black circles) represents the location of the receptive fields of each single afferent fibre in a composite of results from all experiments. cb; celiac branch of the vagus, cg/smp; celiac ganglion and superior mesenteric ganglion.

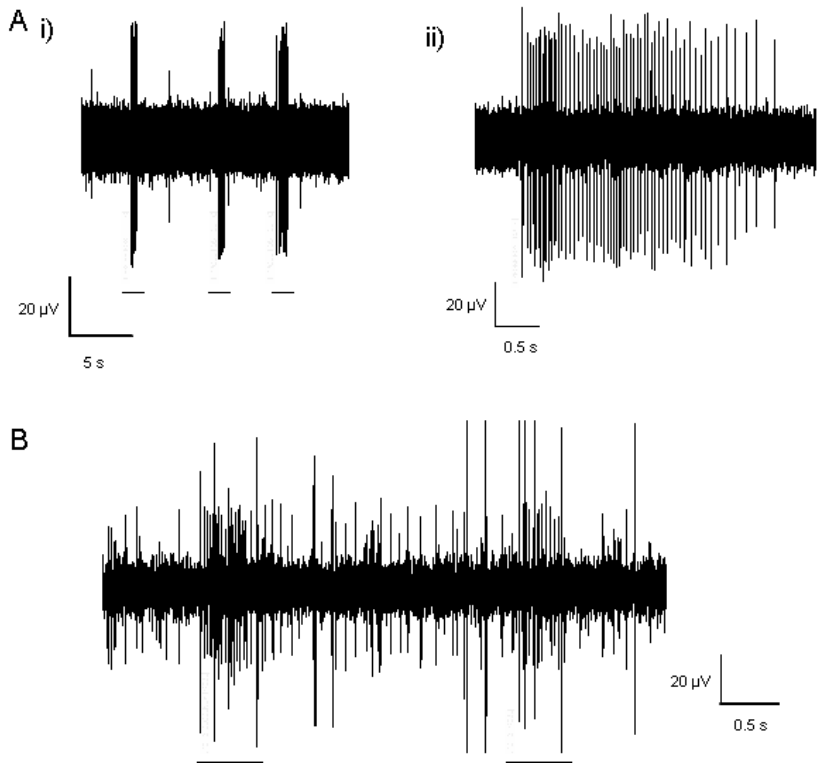

Figure 4.6.5 Responses of rat duodenal vagal afferents to mechanical stimuli.
Raw traces of the electrical activity of single afferent fibres to mechanical stimulation of the duodenum. Duodenal afferent units were identified responses to blunt probing of the serosal surface of the duodenum. A silent duodenal unit activated by probing of the surface of the duodenal tube (A, i). Opening the duodenum longitudinally along the anti-mesenteric border allowed the same unit to be stimulated by a brush on the mucosal surface eliciting a slowly adapting response (ii). This suggests this unit may be a mucosal receptor as it is sensitive to stimulation of the mucosa. Due to rapid degradation of the mucosa in the organ bath the responses of such mucosal units were short-lived, only responding to mechanical stimuli up to a maximum of six times, but generally the response was lost after 2-3 probes. Raw trace showing two single units of different amplitudes (B). The smaller unit, which was spontaneously active, responded to blunt probing (underscored) of the serosal surface of the duodenum. This unit may correspond to previously described tension receptors, responding to stretch created through distortion by the probe. These units tended to show more longevity in eliciting responses to probing (≥ 10 responses).

4.7 Discussion

The studies in this chapter were undertaken to demonstrate a role for GLP-1 in nutrient-evoked reflexes via direct stimulation of gastrointestinal vagal afferents. GLP-1 is released from L-cells in the intestinal epithelium in response to carbohydrate- or fat-rich meals and acts as an enterogastrone, slowing gastric emptying and the transit of further nutrients from the stomach into the intestine as well as reducing further food intake. This action prevents nutrient saturation of the intestine and acts to limit postprandial glycemic excursions. Direct central administration of GLP-1 can experimentally slow gastric emptying (233) however an inhibitory action via peripheral GLP-1 requires an intact vagal afferent pathway (155). GLP-1 regulation of gastric emptying may therefore be mediated via the vagus nerve through activation of GLP-1 receptors on afferent terminals in the periphery. Other gut peptides and mediators released from epithelial enteroendocrine cells, such as cholecystokinin (CCK) and 5-HT, are known to directly stimulate vagal afferents (23, 24, 358, 381) and this afferent activation is an important step in eliciting nutrient-evoked intestinal vagal reflexes. However no direct action of GLP-1 on intestinal vagal afferents has been demonstrated. GLP-1R expression in the nodose ganglion (234) suggests it is probable that afferent endings in the periphery contain the receptor for GLP-1.

To test whether vagal afferents were directly receptive to GLP-1 a validated mouse gastroesophageal preparation for recording single afferent fibres (252) was employed. The properties of gastroesophageal vagal afferents in this isolated preparation have been well established and mechanical stimuli to classify and assess mucosal and tension receptors have been proven to be highly reproducible (254, 255, 326). This isolated preparation, therefore, has the advantage of providing a highly controlled environment to investigate mechanical or chemical properties of vagal afferents. Data from this study showed that GLP-1 did not effect afferent discharge or alter mechanical properties of gastroesophageal vagal afferents as assessed in this preparation.

GLP-1 secreting L-cells are predominantly located in the distal gastrointestinal tract in the jejunum, ileum and colon (84); they are also present in the duodenum, albeit at lower abundance (345). This distal location of L-cells reflects their role in mediating the effects of the 'ileal brake' mechanism where the presence of nutrient in the distal small intestine inhibits upper gut motility and pancreatic secretion preventing nutrient overflow and malabsorption (329, 330, 352, 353). L-cells are not present within the gastric mucosa (282).

The vagus nerve predominantly supplies the thoracic and abdominal cavity, but innervates the entire gastrointestinal tract (17). As a consequence the vagus relays a variety of modalities of sensory information to the CNS through mechano-, chemo- and thermoreceptors and a number of different morphologically specialised afferent endings have been reported (17). The extent of vagal afferent innervation of different regions of the gut suggests that vagal endings are likely to be specialised according to regional requirements. Although GLP-1R expression has been demonstrated in the nodose ganglia, studies have not yet assessed if GLP-1R is expressed in vagal afferents which innervate specific gut regions. Indeed the vagal afferent fibres analysed in this study were predominantly from distal esophagus, and a lack of responsiveness to GLP-1 could be due to esophageal afferents not expressing GLP-1R.

For this reason attempts to investigate vagal afferent responses to GLP-1 in the small intestine were undertaken. An isolated preparation of the rat upper gastrointestinal tract containing the duodenum was adapted for this purpose. GLP-1-secreting L-cells are present in the duodenum (282, 345) and this region may reflect function in the mid-jejunum, where L-cells that co-express $G\alpha_{gust}$ have been identified in rodents (Chapter 3). However difficulty in maintaining the integrity of the duodenal mucosa in this *in vitro* system precluded a systematic investigation of the effects of GLP-1. Other *in vitro* preparations employed to study function of the intestinal mucosa report that duodenal villi are morphologically damaged by 2 hrs and destroyed by 4 hrs (156). The presence of glutamine can increase some parameters of enterocyte health

(367, 368), however the mechanical manipulations required to stimulate and classify vagal afferents and the delivery of GLP-1 in this preparation proved an insurmountable barrier to maintaining mucosal integrity.

Responses of mechanically sensitive duodenal vagal afferents were recorded using this preparation, on occasion. Focal compression of the intact duodenum elicited discharge from afferent receptors. Some units could only be stimulated a few times before the response was lost, presumably due to tissue destruction. Other units maintained responsiveness to probing for longer and were still detected further into the experimental protocol following considerable tissue damage. It seems probable that these types of responses were from intestinal vagal afferents that belong to previously described classes of mucosal and tension receptors found in duodenal recordings *in vivo* (48, 59, 61, 69, 184). Mucosal receptors, so called as their endings are located within the mucosa, respond to mechanical and chemical stimulation of the duodenal mucosa (48, 59, 69). The extremely short-lived responses of some units in this in vitro study are likely to belong to mucosal receptors destroyed during the mucosal damage caused by mechanical stimulation. Indeed on some occasions units did respond to light mucosal stimuli. Tension receptors are known to be located within intestinal muscle layers and are sensitive to distension and light probing (60, 61). Units that had longer lasting evoked responses to distortion of the duodenum in these experiments may have been of this tension receptor type and therefore less vulnerable to mucosal damage.

Due to the nature of the duodenal mucosa an intact blood supply may be necessary to investigate afferent responses of vagal receptors within it. To assess any direct effects of GLP-1 on vagal afferents classification of afferents into receptor types may be important. Previous *in vivo* studies of duodenal vagal afferents show that responses to 5-HT and CCK are specific to mucosal and not tension receptors (22-24). GLP-1 may therefore act in a similar manner on mucosal receptors; however we cannot resolve this from the current dataset.

The mechanisms involved in nutrient signalling via GLP-1 that cause slowing of gastric emptying are likely to be complex. Both peripheral and central sites of action are possible, and the relative contribution of each site has not been established. However, vagal afferent pathways appear to be important for inhibition of motility mediated through peripheral GLP-1. The present studies have demonstrated that mouse esophageal vagal afferents are not directly receptive to GLP-1, however this region does not contain significant populations of L-cells and esophageal vagal afferents are unlikely to be natively exposed to local GLP-1 release. Gastroesophageal vagal afferents however are modulated by other gut peptides. For example by ghrelin, the hunger promoting hormone produced primarily in A cells of the gastric fundus (42, 68, 177), which selectively reduces the mechanosensitivity of gastroesophageal vagal afferents in this preparation (253).

GLP-1 sensitive vagal afferents appear to innervate the portal vein (231, 242, 243) and these increase their firing rate in the presence of GLP-1. GLP-1 detection by vagal afferents in the periphery may occur primarily by vagal endings in the portal vein and not the intestinal mucosa, although GLP-1 in the portal circulation is exposed to and degraded by dipeptidyl peptidase IV (DPP-IV) (234). Recent studies have investigated GLP-1 levels in the intestinal lymph duct after nutrient ingestion and found that levels are five times greater than in the portal vein, while levels of DPP-IV are lower than in plasma (64, 198). These findings may identify the lymph system as a specific conduit of action of GLP-1, although this remains to be investigated further. However it is still likely that intestinal mucosal afferents respond to GLP-1 as they can be activated by other nutrient-released transmitters which inhibit gastric motility. However electrophysiological experiments performed in an *in vivo* animal model with intact mucosa will be required to directly test this hypothesis.